The protective layer formed by soil particles on plastics decreases the toxicity of polystyrene microplastics to earthworms (Eisenia fetida)

Jinbo Liu, Jianjun Qin, Lang Zhu, Kecheng Zhu, Ze Liu, Hanzhong Jia, Eric Lichtfouse

HAL Id: hal-03589788

https://hal.science/hal-03589788

Submitted on 25 Feb 2022

The protective layer formed by soil particles on plastics decreases the toxicity of polystyrene microplastics to earthworms *(Eisenia fetida)*

Jinbo Liu [a], Jianjun Qin [a], Lang Zhu [a], Kecheng Zhu [a], Ze Liu [a], Hanzhong Jia [a,*], Eric Lichtfouse [b]

[a] *Key Laboratory of Plant Nutrition and the Agri-environment in Northwest China, Ministry of Agriculture, College of Natural Resources and Environment, Northwest A & F University, Yangling 712100, China*
[b] *Aix-Marseille Univ, CNRS, IRD, INRA, CEREGE, Aix-en-Provence 13100, France*

ARTICLE INFO

Handling Editor: Adrian Covaci

Keywords:
Polystyrene
Microplastics
Earthworm
Soil
Toxicity
Aging

ABSTRACT

The recent discovery of microplastics contaminants in most ecosystems has raised major health issues, yet knowledge on their impact on soil organisms is limited, especially their toxicity evolution with aging. Here we studied the toxicity of polystyrene microplastic (PS-MP) to earthworm (Eisenia fetida) after aging in soil. Results show that the 50% lethal concentration was 25.67 g kg 1for microplastics, and 96.47 g kg 1 for microplastics that have aged 28 days in soil, indicating that the toxicity of microplastics decreases with aging. Laser scanning confocal microscope and scanning electron microscope (SEM) reveal that the toxicity of microplastics to earthworm may be due to the ingestion of microplastics by earthworms and physical damage, e.g., epidermis abrasion and setae loss. Similarly, the levels of reactive oxygen species, antioxidant enzyme activities and malondialdehyde increased with microplastic concentrations from 0.1 to 1.5 g kg 1, but decreased with aging from 7 to 28 days. The integrated biomarker response index also confirmed that the toxicity of microplastics decreased with aging. SEM reveals that microplastics were progressively covered by soil particles during soil aging, inducing the formation of a protective layer and increasing the particle size of microplastics. This prevented direct contact with earthworms and decreased the ingestion of microplastics and, in turn, decreased microplastic toxicity. Overall, our study provides valuable insights for elucidating the effect of aging on the toxicity of microplastics.

1. Introduction

In the past century, plastics have been widely used in many sectors including coating, wiring, packaging, films, and containers; and up to 32% of that plastics eventually end up in natural environment (Jambeck et al., 2015; Machado et al., 2018a). Plastic debris are broken into fragments in ecosystems by physical, chemical, microbial, and photo-aging processes, inducing the formation of microplastics (MPs) which are defined as particles of size lower than 5 mm (Thompson et al., 2004). MPs can exist in natural environment persistently because of their chemical stability (Li et al., 2021), causing negative effects to ecosystem. On the one hand, MPs themselves can directly cause damages to organisms, resulting in, such as, inflammatory responses, growth inhibition, histological changes, neurotoxicity, and immune toxicity (Diepens and Koelmans, 2018). On the other hand, other xenobiotics which may be adsorbed on MPs due to their high specific surface area could indirectly induce adverse effects (Liu et al., 2020).

MPs are ubiquitous in atmospheric, aquatic, and terrestrial ecosystems (Auta et al., 2017; Wang et al., 2020a; Xu et al., 2020). Ocean has long been considered as the major sink of MPs (Hamer et al., 2014; Watts et al., 2015), and thus, the negative influences of MPs to aquatic organisms, such as plankton, benthic and pelagic animals, have been widely investigated (Rezania et al., 2018). However, recent studies have pointed out that soil is an important sink for MPs which may be more important than marine (Rillig 2012; Sarker et al., 2020). It is estimated that MPs annually discharged to the terrestrial environment is 4–23 times more than those discharged to the marine environment (Horton et al., 2017). Previous studies have reported that the concentrations of MPs in industrial and remote areas can reach 67 g kg^{-1} (Machado et al., 2018b; Zheng et al., 2019). Noteworthy, agricultural land, as an important part of terrestrial ecosystem, is the main sink of MPs due to plastic mulch, application of municipal sewage sludge, and wastewater irrigation (Mahon et al., 2017). For example, around 700,000 tons MPs is estimated to be released into agricultural land in North America and Europe yearly (Nizzetto et al., 2016). It is conceivable that the accumulation of MPs may cause more negative effects in

---

* Corresponding author.
E-mail address: jiahz@nwafu.edu.cn (H. Jia).

soil ecosystems.

After exposing to soil, MPs have impacts on soil quality and soil life activities through altering the physicochemical properties, fertility and microbial communities of soil (Awet et al., 2018; Zhu et al., 2018). Moreover, MPs could lead to the physical damages of tissues and inflammatory response after ingested by many organisms such as snails, nematodes, springtails, collembolan and earthworm (Jeong and Choi 2019; Wang et al., 2020a). The effects of MPs release in soil have attracted more and more attention, however, most of these studies investigate the potential adverse effects with using commercial or pristine MPs. This may lead to the misrepresentation of the risks associated with MPs due to the lack of environmental relevance (Besseling et al., 2014; Watts et al., 2016). Since the characteristics and environmental transformation of MPs influence the risk in environment, virgin MPs, as known, is aged over time in the natural environment (Song et al., 2018) and thus, their physicochemical properties, such as size, shape, and surface chemistry, are changed with aging and further result from the changes of risk of MPs release in soil (Magni et al., 2020). Furthermore, MPs will be adsorbed by soil components (e.g., soil organic carbon and clays) through surface sorption, electrostatic and hydrophobic interactions, which may affect the behaviors and toxicity of MPs in the soil environment (Luo et al., 2020). For instance, Zhu et al. (2020) found that the adsorption and aggregation of Cu^{2+} on MPs was favor for attenuation of the toxicity of copper nanoparticles. Unfortunately, the researches about the ecological impacts of MPs under environmentally relevant exposure conditions is still rare, especially the eco-toxicological effects of MPs in soil over time.

In this study, earthworms (*Eisenia fetida*), the most widespread model organism used to evaluate the toxicity of soil pollutants (OECD, 1984), was chosen as experimental organism to study the toxicity of MPs with taking the process of MPs aging into consideration. Polystyrene microplastic (PS-MP), a commonly produced polymer and the most commonly encountered polymer in the environment (Chae and An, 2018), was selected as model MP. The mortality of PS-MP to earthworms was investigated by 28-day half lethal concentration (LC_{50}), and the possible reasons for the death were explored by analyzing the ingestion of MPs by earthworms and the epidermal damage of MPs to earthworms. In addition, the biochemical indicators associated oxidative stress, including reactive oxygen species (ROS), antioxydant enzymes (e.g., superoxide dismutase (SOD), catalase (CAT), peroxidase (POD) and glutathione-S-transferase (GST)), and malondialdehyde (MDA) (Kim et al., 2008; Gill and Tuteja 2010; Wu et al., 2013; Wang et al., 2017) were systematically investigated to provide critical information to understand the impacts of MPs. Two-way ANOVA was applied to assess influencing factors. And the toxicity of PS-MP to earthworms along with aging was evaluated by integrated biomarker response (IBR). The obtained information would provide a comprehensive theoretical basis for evaluating the environmentally-relevant effects of MPs in terrestrial ecosystem.

2. Materials and methods

2.1. Reagents and PS-MP

Nile Red (>95%) and 2′,7′-dichlorohydro fluorescein diacetate (DCFH-DA, > 97%) were purchased from Aladdin Biochemical Technology Co., Ltd., Shanghai, China. Vermiculite (>99%) was purchased from Benge Mineral Products Co., Ltd., Hebei, China. The beads of pristine PS-MP (500 mesh) were obtained from Dongguan Tesulang Chemical Co., Ltd., Guangdong, China. The solvent-soluble chemicals on PS-MP surface were removed by washing with methanol. The achieved PS-MP were dried at room temperature (~23 °C), and then stored in refrigerator at 4 °C before further analysis and experiment. The properties, including size, composition, metal contents, elemental carbon (EC), organic carbon (OC), and inorganic carbon (IC) of PS-MP were analyzed. Detailed methods are provided in Text S1 (Supplementary

material) and results concerning the size of the PS-MP are provided in Fig. S1. Briefly, the average size of PS-MP is 24.65 ± 5.20 μm, with a OC of 0.92 g g^{-1}. And metals, including Fe, Cu, Zn, Cr, Ni and Mn, are not detected.

2.2. Preparation of soil and earthworms

Soil was collected from the upper 0–20 cm of a cultivated field in the Shaanxi province of China (34°17′N, 108°01′E). The obtained soils were air-dried at ~23 °C, and then sieved through 2 mm. Soil physicochemical properties were analyzed and the detailed methods are provided in Text S2. The collected soil contained 25.48% clay, 57.38% silt, and 17.14% sand, and was with a pH of 7.90. Its organic carbon was 9.56 g kg^{-1} and cation exchange capacity was 22.37 cmol kg^{-1}. Additionally, vermiculite with a size of 3–6 mm was added to soil at a mass percentage of 10% to improve the breathability and water permeability.

Healthy adult earthworms *Eisenia fetida* with a weight of 300–600 mg were obtained from the Hebei Earthworm Breeding Base (Hebei province, China). Before the exposure experiment, earthworms were incubated in the tested soil for 14 days under laboratory conditions.

2.3. Experimental section

The experimental design is shown in Fig. 1, and the specific settings were as follows.

2.3.1. Aging of PS-MP in soil

PS-MP with different aging times were set to study the effect of aging on toxicity. In the acute toxicity, PS-MP was firstly mixed with soil attaining a concentration of 0, 4, 10, 20, 40, 60, 80 and 100 g kg^{-1}, and the mixtures were aging for 7, 14, and 28 days before earthworm exposure. In the subchronic toxicity, the aging experiment included two assays: (i) PS-MP was firstly mixed with soil attaining a concentration of 0–1.5 g kg^{-1}, and the mixtures were aging for 28 days before earthworm exposure; (ii) PS-MP was mixed with soil attaining a concentration of 1.5 g kg^{-1}, and then aging for preselected periods (such as 7, 14, 21, and 28 days) before earthworm exposure.

2.3.2. Acute toxicity

Pot experiments were conducted to investigated the toxicity of PS-MP. In experiment I, PS-MP was added to soil at 0, 4, 10, 20, 40, 60, 80 and 100 g kg^{-1}. The specific setting is provided in Table S1. When PS-MP mixing with soil uniformly, ultra-pure water was added to control the water content of soils at 60%. After the mixture was stabilized for around 2 h, thirty earthworms were added to the pot immediately. The pots were then placed in a climate chamber and cultured at 25 °C with 16 h of light and 8 h of darkness. During the incubation, the water content of soil was controlled at 60% by gravimetric method. Earthworm mortality was monitored after 28 days exposure period.

In experiment II, thirty earthworms were added to 7 days, 14 days and 28 days pre-aged PS-MP, investigating the effects of aging on the acute toxicity. Other steps were the same as above.

2.3.3. Subchronic toxicity

In experiment I, the content of PS-MP was assessed at 0, 0.1, 0.25, 0.5, 1.0 and 1.5 g kg^{-1} based on the 0.25% (w/w) environmental content (Lwanga et al., 2016). The specific setting is provided in Table S2 and each pot contained fifteen earthworms. The earthworms were added to the pot immediately after the PS-MP was mixed evenly with the soil to study the toxicity of PS-MP to earthworms with the cultivation time. The other steps were consistent with the acute toxicity. And earthworms were randomly selected for the assessment of subchronic toxicity indicators at days 7, 14, 21 and 28.

The experiment II was performed to investigate the effects of aging on the subchronic toxicity. In this section, two assays were conducted: (i) earthworms were exposed to 0–1.5 g kg^{-1} 28 days pre-aged PS-MP,
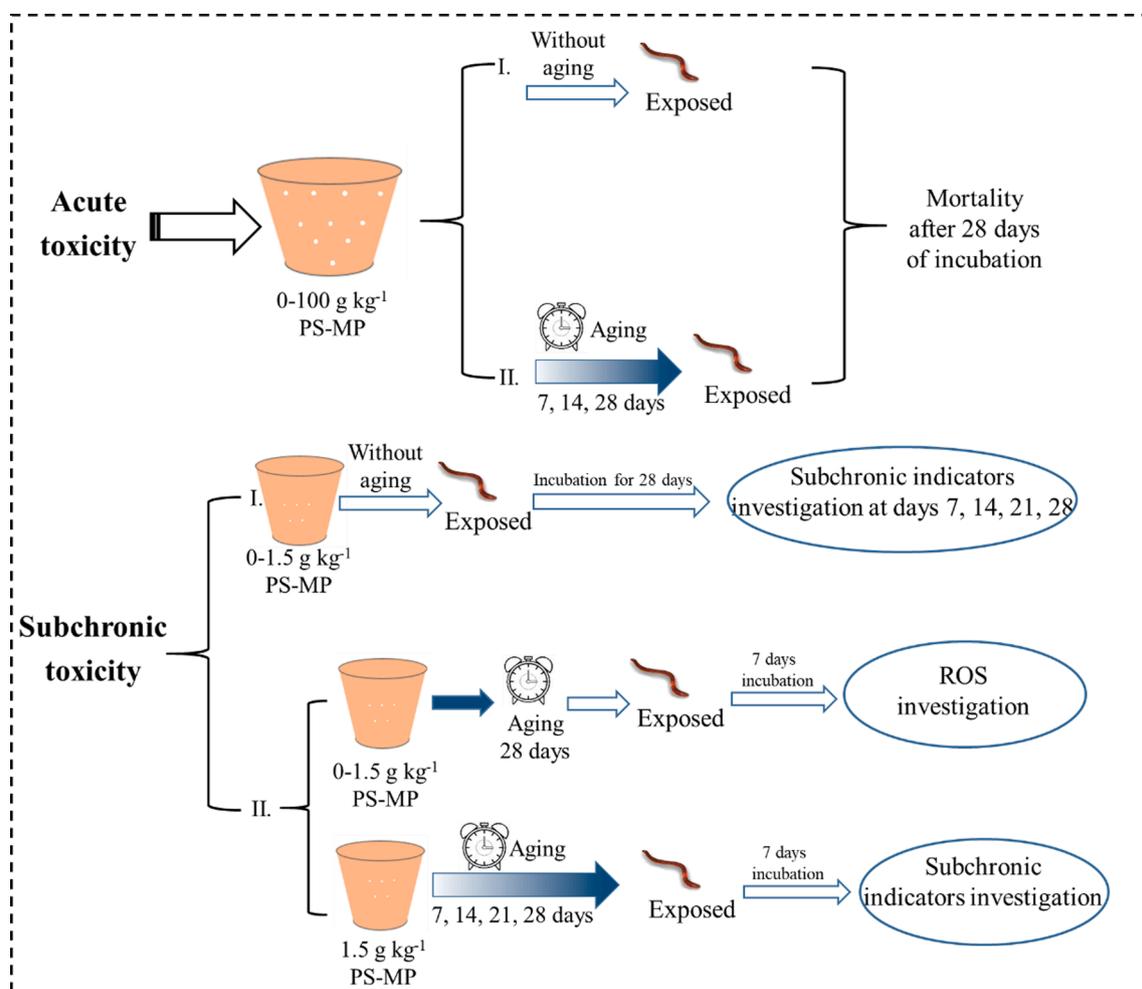
Fig. 1. Experimental design. Pot experiments were performed to investigate the acute and subchronic toxicity of polystyrene microplastic (PS-MP) to earthworms (*Eisenia fetida*), and all these treatments were replicated three times. The exposure concentration of PS-MP in acute and subchronic toxicity is 0–100 g kg^{-1} and 0–1.5 g kg^{-1}, respectively. Both pristine and pre-aged PS-MP were used in acute and subchronic toxicity to study the effect of aging on the toxicity of PS-MP.

and the activity of ROS in earthworm after incubated for 7 days was used to clarify the potential role of aging; (ii) earthworms were added to the pot containing 1.5 g kg^{-1} varied aging periods PS-MP for 7 days, and the subchronic toxicity indicators were investigated to elucidating the effect of aging.

2.3.3.1. Ingestion of PS-MP by earthworms. After exposure to PS-MP for 28 days in experiment I, the method of Erni-Cassola et al. (2017) was used to analyze the presence of PS-MP in earthworm casts and some adjustments were made. The detailed method is provided in Text S3. In addition, the ingestion of aged PS-MP in experiment II was also studied.

2.3.3.2. Physical damage. After exposure to PS-MP for 28 days, the physical damage of earthworm was conducted according to the protocol of Chen et al. (2020). The detailed method is provided in Text S4.

2.3.3.3. ROS activity. The ROS content was assessed using DCFH-DA. Briefly, earthworms were washed, dried, weighed and homogenized in phosphate buffer saline (PBS, 0.1 M, pH = 7.4), and then was centrifuged at 20,000g for 20 min at 4 °C with a TGL-18R Centrifuge, Shandong Baiou Medical Technology Co., Ltd. China. Then the sediment was resuspended in PBS for preparation of the mitochondria suspension, which was mixed with 100 μL DCFH-DA (2 μM) and reacted at 37 °C for 0.5 h. Finally, the reaction mixture was terminated using 200 μL 1 M HCl, and measured by a multifunctional microplate reader (Varioskan

LUX, Thermo Fisher Scientific, USA) with 488 nm (excitation wavelength) and 525 nm (emission wavelength).

2.3.3.4. Antioxidant enzymes activities and MDA content. Consistent with ROS, earthworms were homogenized in PBS and then centrifuged at 3000g for 15 min. And the obtained supernatants were utilized for enzyme assays, such as SOD, CAT, POD, GST and MDA, following the manufacturers' protocol of corresponding assay kit from Suzhou Keming Biotechnology Co., Ltd. (Jiangsu, China).

2.3.3.5. Analysis of PS-MP surface properties. The extraction of PS-MP from soil was conducted following the protocol of Wang et al. (2021) with some modification. The detailed method is provided in Text S5. The obtained PS-MP was examined by scanning electron microscopy (SEM, Nova Nano SEM-450, FEI, USA) to explore the changes in morphology. Energy dispersive spectroscopy was also employed to determine the elemental composition of the particles attached to the surface of PS-MP. In addition, attenuated total reflectance-fourier transform infrared spectroscopy (ATR-FTIR, Thermo Nicolet IS10, Massachusetts, USA) was applied to investigate the PS-MP surface functional groups.

2.4. Statistical analysis

All experiments were repeated for three times and the data were showed as mean ± standard deviation. The LC$_{50}$ of PS-MP to earthworms was evaluated by SPSS 19.0 (SPSS Software, USA), and the

significant differences in biochemical indicators of earthworm among different groups were assessed by one-way analysis of variance (ANOVA) followed by LSD test. Data of biochemical indicators of earthworms after 7 to 28 days exposure to PS-MP under 1.5 g kg^{-1} was selected to calculate IBR index to represent the toxicity over time following the protocol of Sanchez et al. (2013):

Specifically, Y_i is obtained by compare individual average biomarker data (X_i) with average reference data (X_0), in which logarithmic transformation is applied to decrease variance.

$$Y_i = \log(X_i/X_0)$$

By calculating the general mean (μ) and standard deviation (σ) of Y_i, a standardized biomarker response (Z_i) is obtained.

$$Z_i = (Y_i - \mu)/\sigma$$

In order to establish a basal line with 0 as the center and represent the changes of biomarkers based on this baseline, the Z_i and the average of the reference biomarker data (Z_0) are applied to define a biomarker deviation index (A_i).

$$A_i = Z_i - Z_0$$

The absolute value of A_i parameters for each biomarker are summed to obtain integrated biomarker response (IBR).

$$IBR = \sum |A_i|$$

3. Results

3.1. The toxicity of polystyrene microplastics to earthworms

Acute toxicity was tested by adding 0–100 g PS-MP kg^{-1} soil. The mortality of earthworm and the acute toxicity of PS-MP to earthworm are shown in Table 1. As expected, the mortality increased with the concentration of pristine PS-MP, and the 28 d-LC$_{50}$ of pristine PS-MP was 25.67 g kg^{-1} (95% confidence intervals, 19.77–32.62 g kg^{-1}). Interestingly, the mortality in aged PS-MP treatments was lower than in pristine PS-MP at the corresponding PS-MP concentration, although the mortality also increased with the concentration of aged PS-MP. Furthermore, the 28 d-LC$_{50}$ of PS-MP increased to 96.47 g kg^{-1} (95% confidence intervals, 76.64–143.56 g kg^{-1}) after aging for 28 days. These results indicated that the PS-MP toxicity was decreased with aging time.

To explore the possible impact of PS-MP on earthworm, subchonic toxicity was tested by adding 0–1.5 g PS-MP kg^{-1} soil. Results showed the absence of mortality during 28 days (data not shown). We studied the occurrence of PS-MP in earthworm casts and the epidermal injury of earthworm by laser scanning confocal microscope (LSCM) and scanning electron microscope (SEM), respectively (Figs. 2, 3, S2 and S3). Results showed the presence of fluorescent PS-MP in all earthworm casts of PS-MP amended soils, while there were no fluorescent objects in earthworm casts without adding PS-MP (Fig. 2). Moreover, the number of PS-MP in

casts was increasing with PS-MP concentration in soil. Noteworthy, the decrease of the ingestion of PS-MP by earthworms with the increase of PS-MP aging was found in the casts (Fig. S2). The visual phenotype of earthworms showed the physical damage, such as band swelling and pustule, was observed under 1.0 and 1.5 g kg^{-1} PS-MP (Fig. S3 e-f), while no significant damage was found in other treatments (0–0.5 g kg^{-1} PS-MP, Fig. S3 a-d). Consistent with the visual phenotype, SEM results indicated that there was no damage in the control and 0.1–0.5 g kg^{-1} PS-MP treatments (Fig. 3a-h), while multiple setae lacerations and epidermis damage were observed at 1.0 and 1.5 g kg^{-1} PS-MP treatments (Fig. 3i-l).

3.2. Reactive oxygen species in earthworms under microplastic stress

The concentrations of ROS in earthworms of soils amended with PS-MP at 0–1.5 g^{-1} along with incubation time are presented in Fig. 4. Results showed that the highest ROS levels, of 1338.9 fluoe-intensity mg^{-1} Pr, were observed after 7 days for a PS-MP of 1.5 g kg^{-1}, versus 828.6 fluoe-intensity mg^{-1} Pr for the control without PS-MP. ROS levels also increased with the PS-MP concentration. It was worth to note that the induction of ROS versus control decreased with time, from a high induction after 7 days to a low induction after 28 days, indicating the toxicity of PS-MP decreased with aging. To further investigate the toxicity of PS-MP with aging, earthworms were inoculated into the soil within 28-day pre-aged PS-MP and incubated for 7 days. After that, the ROS activity in earthworm was investigated and the results are provided in Fig. S4. We observed that the content of ROS in different treatments was maintained at the same level as the control, indicating the toxicity of PS-MP decreased significantly after aging. Moreover, the ROS content decreased significantly from 1311.6 to 827.6 fluoe-intensity mg^{-1} Pr with the aging of PS-MP prolonged from 7 to 28 days (Fig. S5a), confirming the effect of aging on the decreased toxicity of PS-MP.

3.3. Antioxidant enzymes activities of earthworms under microplastic stress

We measured the activity of antioxydant enzymes, such as SOD, CAT, POD and GST, in earthworms cultivated in soils amended with PS-MP at concentrations of 0–1.5 g kg^{-1}. Results showed that PS-MP induced a sharp increase of SOD concentrations versus the PS-MP free soil, and that SOD concentrations were decreasing with time (Fig. 5). These trends were consistent with the results of ROS (Fig. 4). This meant earthworms highly increase the SOD activity to decrease the high ROS levels after 7 days. The activity of CAT, POD and GST (Figs. S6, S7 and S8) displayed roughly similar trends as SOD, with the higher activities after 7 days and a decreasing activity with time. Enzyme activities globally increased with PS-MP concentration during 14 days of soil in-cubation, yet intriguiging activity decreased occur at 21 and 28 days at high plastic concentrations. In addition, the difference in the activity of SOD, CAT, POD and GST decreased with aging (Fig. S5b-e).

Table 1
The mortality and acute toxicity of PS-MP to earthworms.

Concentration of PS-MP (g·kg^{-1})	Initial earthworm number	Deaths day 28			
		Pristine PS-MP	7-day aged PS-MP	14-day aged PS-MP	28-day aged PS-MP
100	30	29 ± 0	25 ± 1	20 ± 0	16 ± 2
80	30	24 ± 2	21 ± 1	17 ± 1	12 ± 2
60	30	22 ± 1	18 ± 1	14 ± 0	9 ± 1
40	30	17 ± 2	13 ± 0	8 ± 1	5 ± 1
20	30	11 ± 1	9 ± 0	6 ± 0	2 ± 0
10	30	7 ± 1	4 ± 0	2 ± 0	0 ± 0
4	30	3 ± 0	1 ± 0	0 ± 0	0 ± 0
0	30	0 ± 0	0 ± 0	0 ± 0	0 ± 0
28 d-LC$_{50}$ (g·kg^{-1})		25.67 (19.77–32.62) [a]	40.48 (31.86–51.98) [a]	65.49 (51.66–89.43) [a]	96.47 (76.64–143.56) [a]

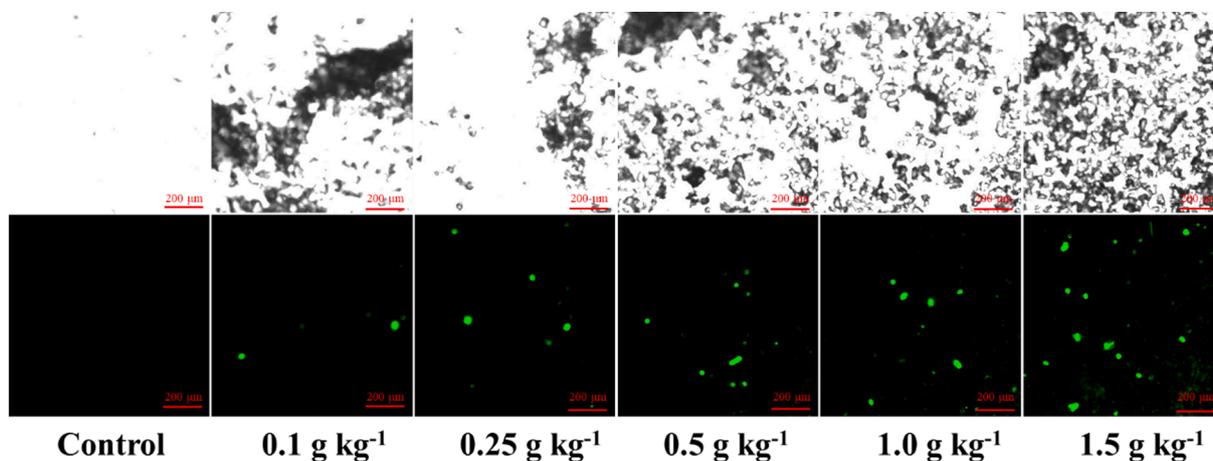[a] The values in bracket represent 95% confidence intervals of the mean.

Fig. 2. Images of polystyrene microplastic (PS-MP) collected from earthworm casts stained with Nile red in bright field and green fluorescence (excitation and emission at 561 and 570–670 nm, respectively) after exposure to PS-MP for 28 days. The green dots were PS-MP, which increased with the concentration of PS-MP.
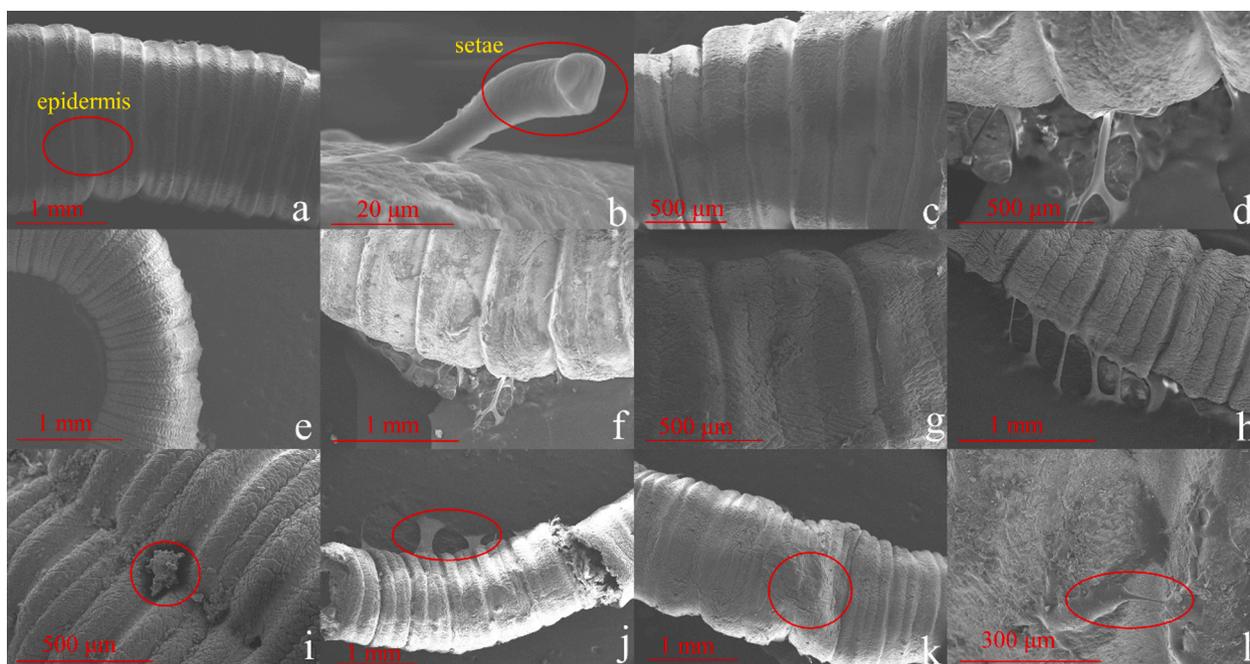

Fig. 3. Scanning electron microscope (SEM) images of the physical damage of earthworms after exposure to 0 g kg^{-1} (a, b, control), 0.1 g kg^{-1} (c, d), 0.25 g kg^{-1} (e, f), 0.5 g kg^{-1} (g, h), 1.0 g kg^{-1} (i, j), 1.5 g kg^{-1} (k, l) polystyrene microplastic (PS-MP) for 28 days. Note the occurrence of surface abrasion, lacerations of the epidermis and loss of setae at 1.0 (i, j) and 1.5 g kg^{-1} (k, l) PS-MP.

3.4. Assessment of the biological toxicity of microplastics during incubation period

The changes in malondialdehyde (MDA) was determined to evaluate oxidative damage (Fig. 6). Consistent to the trend of ROS and antioxidant en-zymes, PS-MP induce a significant increase of MDA concentrations versus control at day 7, and that decreased with time. MDA contents in PS-MP amended soils were at the control level on day 28. In addition, the difference in the content of MDA also decreased with the aging of PS- MP (Fig. S5f).

Two-way ANOVA (Table S3) results showed that the test biomarkers was significantly influenced by both dose and time ($p <$ 0.05), except for CAT as function of dose. Post hoc test using LSD after two-way ANOVA (Table S4) indicated that the exposure times significant affected the response of biomarkers, indicating aging plays an important role in the toxicity of PS-MP. Integrated biomarker response (IBR) index is applied to further assess the biological toxicity of PS-MP with aging (Sanchez

et al., 2013). The IBR index histogram and a star plot under 1.5 g kg^{-1} PS-MP concentration from day 7 to 28 are shown in Fig. 7. The IBR index decreased from 15.64 to 13.12, which indicated that the toxicity of PS-MP decreased with aging (Fig. 7a). In addition, the IBR index decreased significantly from 11.94 to 4.10 with the aging of PS-MP prolonged from 7 to 28 days (Fig. S5g). These results were in accordance with the obtained results of ROS, antioxydant enzymes and MDA. The responses of the biomarkers in the star plot showed that the toxicity effects were manifested by the increase in the content of ROS, SOD and MDA, and the inhibition of the activity of POD and GST (Fig. 7b).

3.5. Characterization of aging microplastics

To clarify the mechanism by which toxicity decreased with aging, the analysis and characterization of aged PS-MP, such as SEM, ATR-FTIR, and particle size, were investigated. The SEM images showed that the pristine PS-MP were spherical particles with a smooth surface (Fig. 8a-
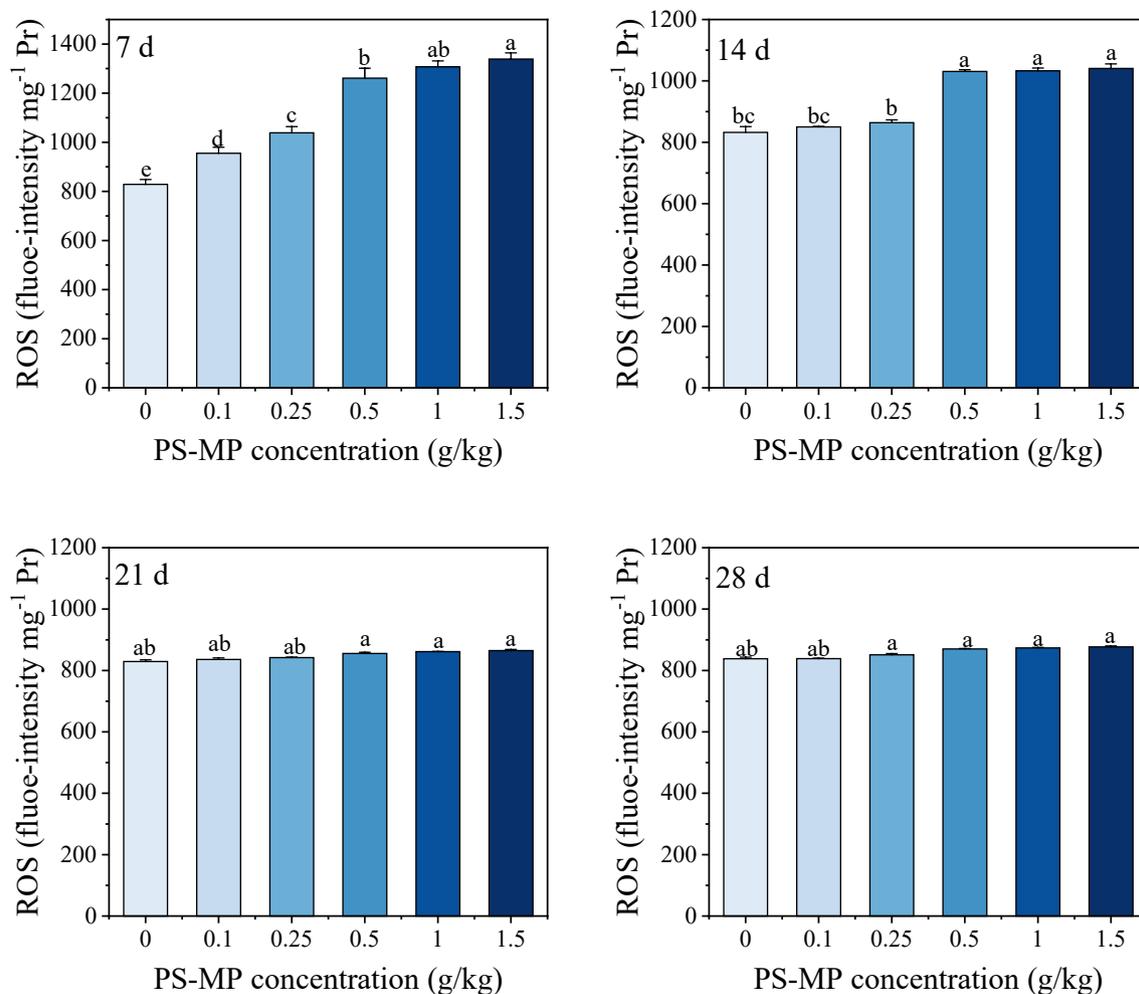
Fig. 4. The concentration of reactive oxygen species (ROS) in earthworms after 7, 14, 21, 28 days exposure to polystyrene microplastic (PS-MP) at various concentrations. Note the high induction of ROS and the increase of ROS with the PS-MP concentration on day 7; and the decrease induction of ROS with time. The values are presented as the mean ± SD (n = 3), and the error bars represent the standard deviation. Different letters above columns indicate significant differences at $p < 0.05$ level among treatments.

b). After aging, the morphology of PS-MP particles changed from smooth to rough (Fig. 8c-j), indicating that PS-MP was encapsulated by soil particles. For example, some fine particles were adsorbed on the surface of PS-MP after aging in soil for 7 days (Fig. 8c-d). With the extension of aging, the surface of PS-MP was wrapped by sheet (Fig. 8e-f) and biofilm-like soil particles (Fig. 8g-h). After 28 days of aging, the PS-MP was wrapped by soil particles (Fig. 8i-j). SEM-EDX elemental analysis indicated that the particles on PS-MP surface were primarily composed of O, Fe and Mn (Fig. S9) that increased with aging (Table S5). ATR-FTIR showed that the peak intensities of C=C group at 1601 cm^{-1} decreased with aging compared to the pristine PS-MP (Fig. S10). In addition, the peak intensities of C—OH group at 3740 and 930 cm^{-1} and C—O group at 1230 and 1067 cm^{-1} increased with aging compared to the pristine PS-MP. In addition, the particle size of PS-MP increased from 27.40 ± 2.80 to 33.79 ± 5.00 μm with the aging increased from 7 to 28 days (Fig. S11).

4. Discussion

4.1. Toxic effects of microplastics on earthworms

Acute test can reflect the toxicity of substances simply and quickly, and make a preliminary estimation on the ecological toxicity (OECD, 1984). LC$_{50}$ is an important parameter to measure the toxicity of

toxicants to animals and even humans, and it can provide an objective determination of death effect (Wang et al., 2020b). Compared with conventional pollutants, the higher LC$_{50}$ (25.67 g kg^{-1}) of PS-MP indicated that PS-MP has a lower level of acute toxicity. For example, the LC$_{50}$ of weak base carbendazim to earthworm (*Eisenia fetida*) in five types soils was in the range of 2.32–34.0 mg kg^{-1} (Liu et al., 2012). In addition, considering the real concentration of MPs (0.25% w/w) in soils (Lwanga et al., 2016), we speculate that PS-MP has little acute toxicity to earthworms. This was consistent with the results of our subchronic experiment, which had no mortality of earthworm. More importantly, the increase of LC$_{50}$ for aged PS-MP indicated that the toxicity of PS-MP tended to be decreased with the process of MPs aging.

The toxic effects of PS-MP to earthworms may be attributed to two aspects. On the one hand, earthworms (*Eisenia fetida*) mainly intake organic substances that are easily available in the soil. MPs are almost entirely composed of organic carbon and thus may be ingested by earthworms, inducing negative effects. For instance, Chen et al. (2020) found that MPs with particle sizes smaller than 300 μm could be ingested by *Eisenia fetida*. The size of PS-MP used in this study was 24.65 ± 5.20 μm, and this indicated the possibility of PS-MP being ingested by earthworm. Our findings also confirmed that PS-MP could be ingested and accumulated by *Eisenia fetida* due to the feeding behavior of earthworms. On the other hand, the abrasion of the earthworm surface by the plastics is able to cause adverse impacts. Rodriguez-Seijo et al.
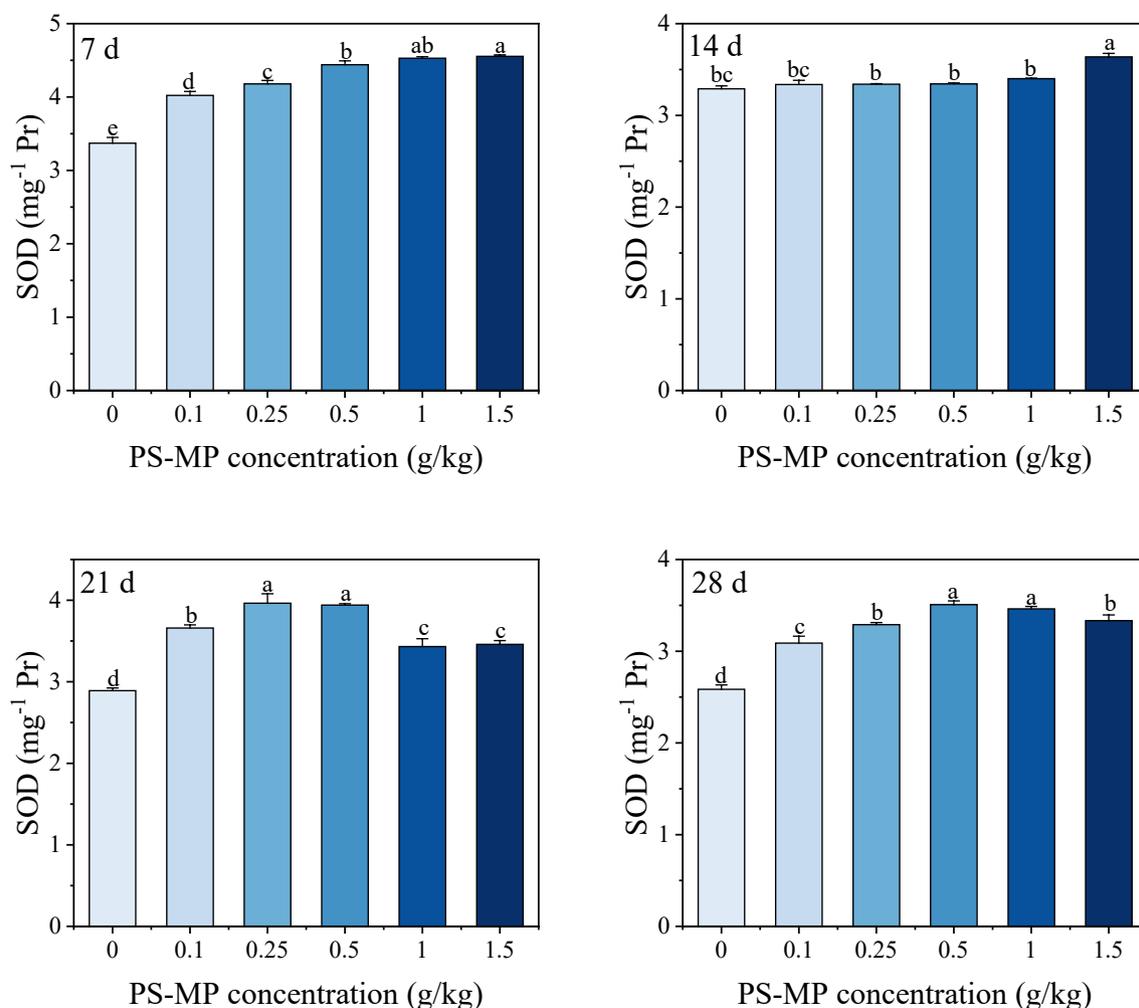
Fig. 5. The superoxide dismutase (SOD) activity in earthworms after 7, 14, 21, 28 days exposure to polystyrene microplastic (PS-MP) at various concentrations in soils. Note the increase of SOD with PS-MP concentration; and the decrease of SOD with time. The values are presented as the mean ± SD (n = 3), and the error bars represent the standard deviation. Different letters above columns indicate significant differences at $p < 0.05$ level among treatments.

(2017) reported that the physical damage of *Eisenia andrei* was slight when the concentration of polyethylene pellets was 62.5 mg kg^{-1} soil$_{dw}$, whereas damage was severe when polyethylene increased to 1000 mg kg^{-1}. Similarly, the physical damage, such as setae lacerations and epidermis damage, were observed at PS-MP with higher concentration treatments (1.0 and 1.5 g kg^{-1}) in the present study. These organs are favored to the movement of the earthworm, playing a pivotal role in the health of earthworms. Overall, the toxic effect of PS-MP on earthworm may be explained by the ingesting PS-MP incidentally lead to external or/and internal mechanical injuries, ulceration, and blockages of the digestive tract or/and attaching PS-MP to the body induce physical damage.

4.2. Responses of earthworms to microplastics

Upon addition of a contaminant, the content of ROS rises and simultaneously, induces oxidative stress in organism (Wu et al., 2013). Previous studies reported the ROS increase was induced by MPs in aquatic organisms, and by polyethylene and polypropylene in earthworms (Wang et al., 2020c; Li et al., 2021). Similarly, our findings also revealed that PS-MP leaded to the accumulation of ROS and thus a strong oxidative stress in earthworms on day 7. After that, the induction of ROS decreased and returned to the same level of control, indicating the decrease of oxidative stress. Several hypotheses may be proposed to explain this decline of oxidative stress with time. First, earthworm may

have adapted to the toxicity, but this seems unlikely in a such short time by a slow evolving organism, versus microbes for instance. Second, the toxicity of MPs may decrease with aging under the soil conditions. Specifically, the MPs surface may be rapidly covered by water, microbes, humic substances and minerals, thus forming a protective layer. This is supported by the well-known soil-pollutant aging phenomenon, by which the bioavailability of pollutant is decreasing with time, yet underlying mechanisms are still poorly known (Reid et al., 2000). The protective layer hypothesis is also supported by the format of very resistant organic residues, termed ultralaminae, in soils (Lichtfouse et al, 1996). Last, a recent study shows that MPs debris dumps have created biodiversity hotspots in deep-sea canyons (Song et al., 2021), which supports indirectly the fact that the surface of aged plastics is not or slightly toxic, as a possible result of the formation of a protective layer.

Antioxidant enzymes, such as SOD, CAT, POD and GST, play a pivotal role in eliminating excess ROS in organisms (Qu et al., 2010; Jia et al., 2014). SOD eliminates the superoxide anion (O$_2$$^{\cdot-}$) by converting O$_2$$^{\cdot-}$ into H$_2$O$_2$ and O$_2$; CAT and POD detoxify organisms by convert H$_2$O$_2$ into water and oxygen; GST, scavenge the metabolites of lipid peroxidation and in turn reduce oxidative damage (Wu et al., 2011). In the present study, almost all of the activity of SOD, CAT, POD and GST in earthworm increased notably after exposed to PS-MP for 7 days. After that, the activity of these enzymes decreased on day 28, and most of them were significantly inhibited. Previous studies report that exposure to MPs can upregulate the content of ROS, thus perturbing the
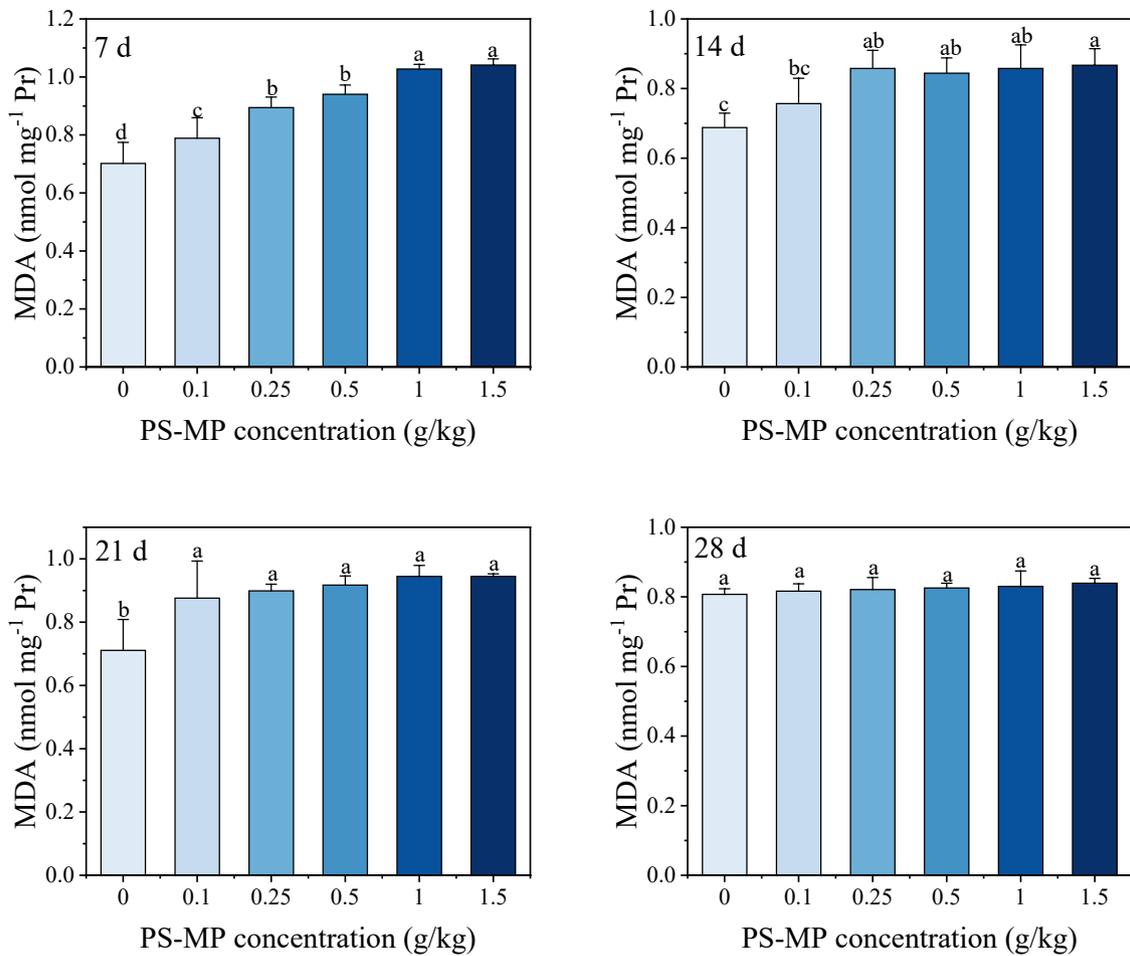
Fig. 6. Lipid peroxidation monitored using malondialdehyde (MDA) content in earthworms incubated 7–28 days in soils amended with polystyrene microplastic (PS-MP). Note that lipid peroxidation is increased with PS-MP concentration on day 7, then decreases with incubation time. The values are presented as the mean ± SD (n = 3), and the error bars represent the standard deviation. Different letters above columns indicate significant differences at $p < 0.05$ level among treatments.
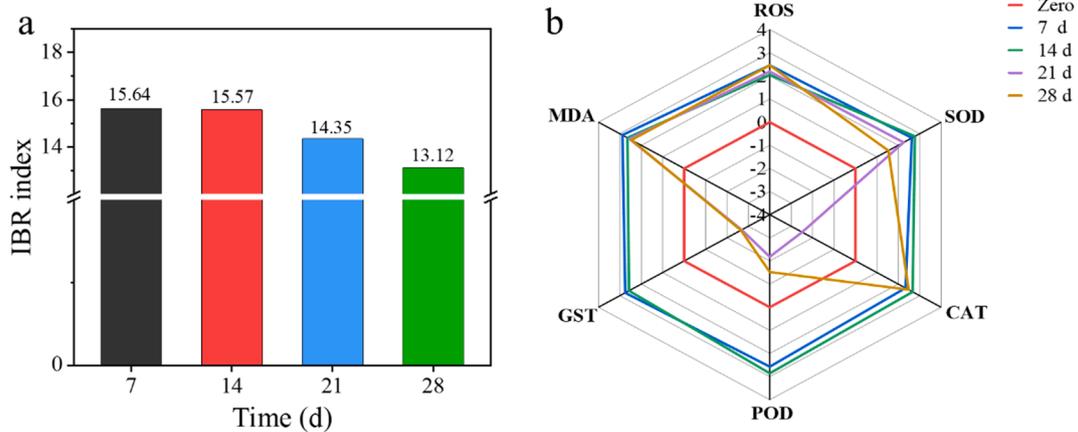

Fig. 7. Integrated biomarker response (IBR) index (a) and star plot (b) of 1.5 g kg^{-1} PS-MP from day 7 to 28 exposure. (In the star plot, above zero means activation or increase, below zero means inhibition or decrease.)

antioxidant system (Li et al., 2021). As the first line of defense against ROS, changes in SOD activity indicated that exposure to PS-MP could induce antioxidant defenses in earthworm. Exposure to PS-MP initially resulted in the accumulation of ROS (day 7, Fig. 4), which then stimulated the biosynthesis of antioxidant enzymes on day 7. After that, the global decrease of antioxidant enzymes level with time was most probably due to the decline in the accumulation of ROS induced by

decrease of toxicity of PS-MP in soils as the result of aging, e.g., by possible formation of a protective layer around MPs particles. Interestingly, the activity of enzyme, including CAT, POD and GST, in high plastic concentrations (1.0 and 1.5 g kg^{-1}) was much lower than the plastic-free soil on day 21 and 28. Here we suspected that the higher concentration and surface of MPs may have induced a higher surface of protective layer containing organics, minerals and microbes, which may
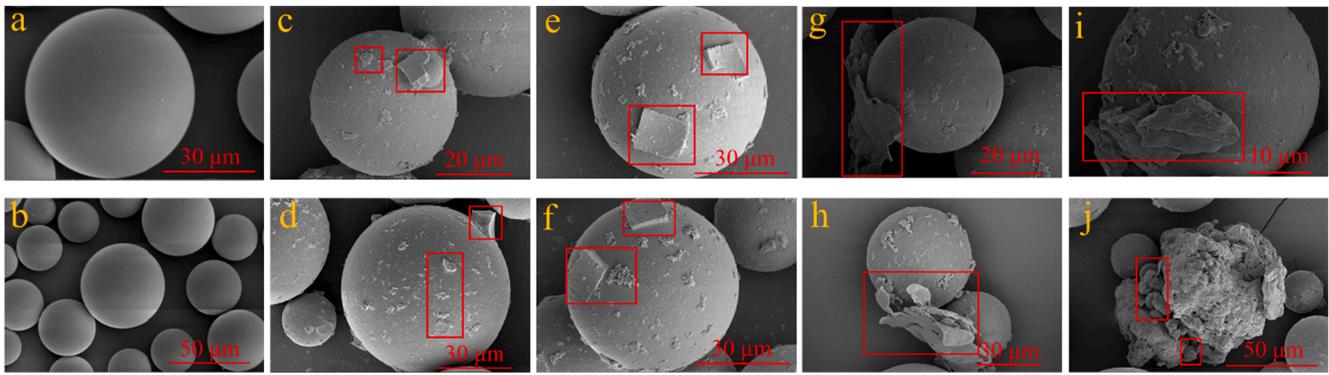
Fig. 8. SEM images of pristine (a, b), aging for 7 days (c, d), 14 days (e, f), 21 days (g, h) and 28 days (i, j) polystyrene microplastic (PS-MP) particals. The morphology of PS-MP changed from smooth to rough with aging, indicating PS-MP was wrapped by soil particles to form the protective layer.

further reduce the toxicity of PS-MP. This supported our hypothesis of a protective layer around plastic particles because more plastic would induce more protective layer surface and, in turn, less toxicity.

When antioxidant defenses fail to eliminate excess ROS, free radicals can affect the structure and function of biomacromolecules, such as membrane lipids, which can be monitored by rises in the concentrations of MDA (Gill and Tuteja, 2010; Shi and Zhou 2010; Shao et al., 2018). The increase of MDA content indicated the occurrence of oxidative damage. Our results showed that MDA in PS-MP amended soils was significantlt higher than PS-MP free soil on day 7, and the MDA increased with PS-MP concentration. The exacerbation of lipid peroxidation may be ascribed to the rate of antioxidant and detoxification enzyme production could not accommodate the increases in ROS (Hackenberger et al., 2018). However, MDA decreased with aging and gradually returned to baseline levels, this was a result of the joint action of ROS and antioxidant enzymes. Moreover, the decrease of MDA with aging indicated that the toxicity of PS-MP was decreased, supporting our hypothesis of a protective layer around PS-MP, which in turn reduce the toxicity of PS-MP.

4.3. The protective layer of soil particles relieves plastic stress to earthworms

The interaction between PS-MP and soil particles in the soil environment may induce the formation of protective layers, and thus decrease the toxicity of PS-MP. SEM images indicated that PS-MP was gradually wrapped by soil particles forming protective layer. SEM-EDX elemental analysis showed that the particles could be minerals

containing oxygen, iron and manganese, such as organic matter, iron oxide and manganese oxide. ATR-FTIR showed that oxygen-containing functional groups was able to be formed on PS-MP during the aging process (Gao et al., 2018). Zhu et al. (2019) also reported that the photoaging induced more oxygen-containing functional groups on PS-MP; however, due to the lack of physicochemical action, the aging of PS-MP in soill is slower than that of photoaging (Machado et al., 2018b). This indicates that the oxygen-containing functional groups on PS-MP may be organic matter or oxidized minerals adsorbed on the surface of PS-MP, which leads to the formation of protective layer. In addition, the increase in the particle size of PS-MP with aging also indicated the formation of protective layer and this could explain the decrease of PS-MP uptake by earthworms. Overall, our findings and literature observations are supported by the following scenario (Fig. 9): at earlier stage of incubation, the surface of PS-MP particles is mostly free. Then, with increasing soil incubation, a biofilm-like protective layer is forming around PS-MP particles (Amaral-Zettler et al., 2020; Yang et al., 2020; Zhou et al., 2021). And the decreased toxicity of PS-MP with aging could be ascribed to two aspects. On the one hand, the formed protective layer protected the PS-MP toxic moieties, such as benzene, and styrene, from direct contact with earthworms. On the other hand, the wrapping effect of soil particles to PS-MP increased the particle size of PS-MP, which in turn decreased the ingestion of PS-MP by earthworm.

5. Conclusion

The present study clearly demonstrated that PS-MP caused negative effects in earthworms initially, but the aging of MPs decreased the
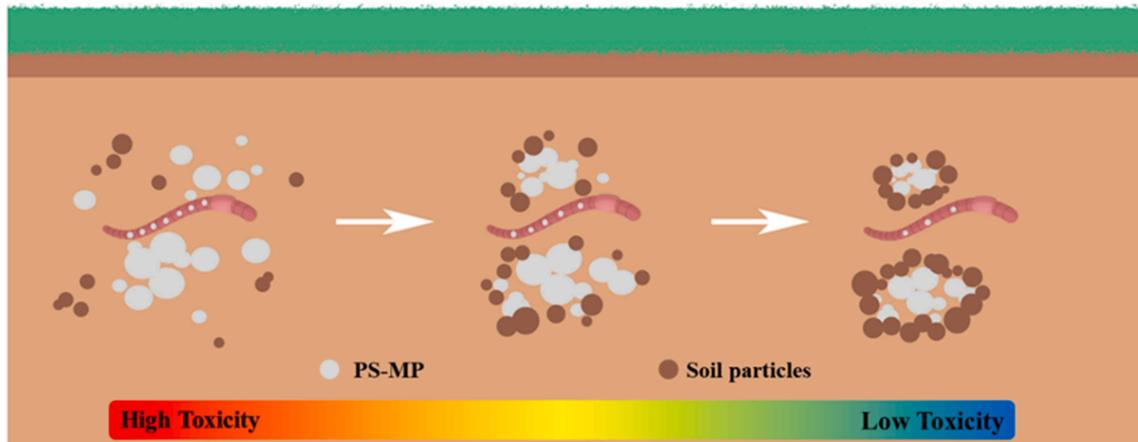

Fig. 9. The scheme of aging on the toxicity of polystyrene microplastic (PS-MP) to earthworms. At the initial, earthworms can direct contact of the PS-MP surface and ingestion PS-MP, exhibiting high toxicity. Along with aging, PS-MP was wrapped by soil particles, which induced the formation of protective layer and increasd the particle size of PS-MP. This protected earthworms from direct contact with PS-MP, and decrease the ingestion of PS-MP, exhibiting low toxicity.

toxicity of PS-MP by formation of a protective layer on the surface of MPs. Our study confirmed that although PS-MP was initially toxic to earthworms, this effect could be reduced by the process of MPs aging. This result was different from most previous reports, which suggesting that the risks of MPs have been somewhat exaggerated. Further investigations are needed to consider long-term aging on the impact of physicochemical properties of MPs and of interface interaction between MPs and soil components, especially these effects on the environmentally-relevant effects of MPs.

CRediT authorship contribution statement

Jinbo Liu: Conceptualization, Investigation, Formal analysis, Writing – original draft. **Jianjun Qin:** Writing – review & editing. **Lang Zhu:** Formal analysis. **Kecheng Zhu:** Writing – review & editing. **Ze Liu:** Validation, Writing – review & editing. **Hanzhong Jia:** Conceptualization, Resources, Supervision, Writing – review & editing, Funding acquisition. **Eric Lichtfouse:** Conceptualization, Investigation, Writing – review & editing.

Declaration of Competing Interest

The authors declare that they have no known competing financial interests or personal relationships that could have appeared to influence the work reported in this paper.

Acknowledgements

Appendix A. Supplementary material

Supplementary data to this article can be found online at https://doi.org/10.1016/j.envint.2022.107158.

References

Auta, H.S., Emenike, C.U., Fauziah, S.H., 2017. Distribution and importance of microplastics in the marine environment: A review of the sources, fate, effects, and potential solutions. Environ. Int. 102, 165–176. https://doi.org/10.1016/j.envint.2017.02.013.

Awet, T.T., Kohl, Y., Meier, F., Straskraba, S., Grün, A.-L., Ruf, T., Jost, C., Drexel, R., Tunc, E., Emmerling, C., 2018. Effects of polystyrene nanoparticles on the microbiota and functional diversity of enzymes in soil. Environ. Sci. Eur. 30 (1) https://doi.org/10.1186/s12302-018-0140-6.

Amaral-Zettler, L.A., Zettler, E.R., Mincer, T.J., 2020. Ecology of the plastisphere. Nat. Rev. Microbiol. 18, 139–151. https://doi:10.1038/s41579-019-0308-0.

Besseling, E., Wang, B.o., Lürling, M., Koelmans, A.A., 2014. Nanoplastic affects growth of S. obliquus and reproduction of D. magna. Environ. Sci. Technol. 48 (20), 12336–12343. https://doi.org/10.1021/es503001d.

Chae, Y., An, Y.J., 2018. Current research trends on plastic pollution and ecological impacts on the soil ecosystem: a review. Environ. Pollut. 240, 387–395. https://doi.org/10.1016/j.envpol.2018.05.008.

Chen, Y., Liu, X., Leng, Y., Wang, J., 2020. Defense responses in earthworms (Eisenia fetida) exposed to low-density polyethylene microplastics in soils. Ecotoxicol. Environ. Saf. 187, 109788. https://doi.org/10.1016/j.ecoenv.2019.109788.

Diepens, N.J., Koelmans, A.A., 2018. Accumulation of plastic debris and associated contaminants in aquatic food webs. Environ. Sci. Technol. 52 (15), 8510–8520. https://doi.org/10.1021/acs.est.8b02515.

Erni-Cassola, G., Gibson, M.I., Thompson, R.C., Christie-Oleza, J.A., 2017. Lost, but found with Nile red: a novel method for detecting and quantifying small microplastics (1 mm to 20 μm) in environmental samples. Environ. Sci. Technol. 51 (23), 13641–13648. https://doi.org/10.1021/acs.est.7b04512.

Gill, S.S., Tuteja, N., 2010. Reactive oxygen species and antioxidant machinery in abiotic stress tolerance in crop plants. Plant Physiol. Biochem. 48 (12), 909–930. https://doi.org/10.1016/j.plaphy.2010.08.016.

Gao, P., Yao, D., Qian, Y., Zhong, S., Zhang, L., Xue, G., Jia, H., 2018. Factors controlling the formation of persistent free radicals in hydrochar during hydrothermal

conversion of rice straw. Environ. Chem. Lett. 16 (4), 1463–1468. https://doi.org/10.1007/s10311-018-0757-0.

Hackenberger, D.K., Stjepanovic, N., Loncaric, Z., Hackenberger, B.K., 2018. Acute and subchronic effects of three herbicides on biomarkers and reproduction in earthworm, Dendrobaena veneta. Chemosphere 208, 722–730. https://doi.org/10.1016/j.chemosphere.2018.06.047.

Horton, A.A., Walton, A., Spurgeon, D.J., Lahive, E., Svendsen, C., 2017. Microplastics in freshwater and terrestrial environments: Evaluating the current understanding to identify the knowledge gaps and future research priorities. Sci. Total Environ. 586, 127–141. https://doi.org/10.1016/j.scitotenv.2017.01.190.

Hamer, J., Gutow, L., Kohler, A., Saborowski, R., 2014. Fate of Microplastics in the Marine lsopod Idotea emarginata. Environ. Sci. Technol. 48, 13451–13458. https://doi.org/10.1021/es501385y.

Jambeck, J.R., Geyer, R., Wilcox, C., Siegler, T.R., Perryman, M., Andrady, A., Narayan, R., Law, K.L., 2015. Plastic waste inputs from land into the ocean. Science 347 (6223), 768–771.

Jeong, J., Choi, J., 2019. Adverse outcome pathways potentially related to hazard identification of microplastics based on toxicity mechanisms. Chemosphere 231, 249–255. https://doi.org/10.1016/j.chemosphere.2019.05.003.

Jia, H.H., Sun, R.J., Shi, W.N., Yan, Y., Li, H., Guo, X.Q., Xu, B.H., 2014. Characterization of a mitochondrial manganese superoxide dismutase gene from Apis cerana cerana and its role in oxidative stress. J. Insect Physiol. 60, 68–79. https://doi.org/10.1016/j.jinsphys.2013.11.004.

Kim, J., Takahashi, M., Shimizu, T., Shirasawa, T., Kajita, M., Kanayama, A., Miyamoto, Y., 2008. Effects of a potent antioxidant, platinum nanoparticle, on the lifespan of Caenorhabditis elegans. Mech. Ageing Dev. 129 (6), 322–331. https://doi.org/10.1016/j.mad.2008.02.011.

Luo, Y., Zhang, Y., Xu, Y., Guo, X., Zhu, L., 2020. Distribution characteristics and mechanism of microplastics mediated by soil physicochemical properties. Sci. Total Environ. 726, 138389. https://doi.org/10.1016/j.scitotenv.2020.138389.

Huerta Lwanga, E., Gertsen, H., Gooren, H., Peters, P., Salánki, T., van der Ploeg, M., Besseling, E., Koelmans, A.A., Geissen, V., 2016. Microplastics in the terrestrial ecosystem: implications for Lumbricus terrestris (Oligochaeta, Lumbricidae). Environ. Sci. Technol. 50 (5), 2685–2691. https://doi.org/10.1021/acs.est.5b05478.

Li, B., Song, W., Cheng, Y., Zhang, K., Tian, H., Du, Z., Wang, J., Wang, J., Zhang, W., Zhu, L., 2021. Ecotoxicological effects of different size ranges of industrial-grade polyethylene and polypropylene microplastics on earthworms Eisenia fetida. Sci. Total Environ. 783, 147007. https://doi.org/10.1016/j.scitotenv.2021.147007.

Liu, K.L., Pan, X., Han, Y.L., Tang, F.F., Yu, Y.L., 2012. Estimating the toxicity of the weak base carbendazim to the earthworm (Eisenia fetida) using in situ pore water concentrations in different soils. Sci. Total Environ. 438, 26–32. https://doi.org/10.1016/j.scitotenv.2012.08.008.

Liu, P., Lu, K., Li, J., Wu, X., Qian, L.i., Wang, M., Gao, S., 2020. Effect of aging on adsorption behavior of polystyrene microplastics for pharmaceuticals: Adsorption mechanism and role of aging intermediates. J. Hazard. Mater. 384, 121193. https://doi.org/10.1016/j.jhazmat.2019.121193.

Lichtfouse, É., Chenu, C., Baudin, F., 1996. Resistant ultralaminae in soils. Org Geochem. 25 (3-4), 263–265. https://doi.org/10.1016/S0146-6380(96)00126-X.

Magni, S., Bonasoro, F., Della Torre, C., Parenti, C.C., Maggioni, D., Binelli, A., 2020. Plastics and biodegradable plastics: Ecotoxicity comparison between polyvinylchloride and Mater−Bi (R) micro−debris in a freshwater biological model. Sci. Total Environ. 720, 137602 https://doi.org/10.1016/j.scitotenv.2020.137602.

de Souza Machado, A.A., Lau, C.W., Till, J., Kloas, W., Lehmann, A., Becker, R., Rillig, M.C., 2018. Impacts of microplastics on the soil biophysical environment. Environ. Sci. Technol. 52 (17), 9656–9665. https://doi.org/10.1021/acs.est.8b02212.

Souza Machado, A.A., Kloas, W., Zarfl, C., Hempel, S., Rillig, M.C., 2018. Microplastics as an emerging threat to terrestrial ecosystems. Glob. Change Biol. 24 (4), 1405–1416. https://doi.org/10.1111/gcb.14020.

Mahon, A.M., O`Connell, B., Healy, M.G., O`Connor, I., Officer, R., Nash, R., Morrison, L., 2017. Microplastics in Sewage Sludge: Effects of Treatment. Environ. Sci. Technol. 51 (2), 810–818. https://doi.org/10.1021/acs.est.6b04048.

Nizzetto, L., Langaas, S., Futter, M., 2016. Do microplastics spill on to farm soils? Nature 537, 488. https://doi.org/10.1038/537488b.

OECD, 1984. The Current Organization of Economic and Cooperative Development Acute Earthworm Toxicity Test (OECD). Guidelines for the Testing of Chemicals, No. 207, Earthworm Acute Toxicity Tests.

Qu, B., Zhao, H., Zhou, J., 2010. Toxic effects of perfluorooctane sulfonate (PFOS) on wheat (Triticum aestivum L.) plant. Chemosphere 79 (5), 555–560. https://doi.org/10.1016/j.chemosphere.2010.02.012.

Thompson, R.C., Olsen, Y., Mitchell, R.P., Davis, A., Rowland, S.J., John, A.W., McGonigle, D., Russell, A.E., 2004. Lost at sea: Where is all the plastic? Science 304, 838. https://doi.org/10.1126/science.1094559.

Rillig, M.C., 2012. Microplastic in terrestrial ecosystems and the soil? Environ. Sci. Technol. 46 (12), 6453–6454. https://doi.org/10.1021/es302011r.

Rezania, S., Park, J., Din, M.M., Taib, S.M., Talaiekhozani, A., Yadav, K.K., Kamyab, H., 2018. Microplastics pollution in different aquatic environments and biota: A review of recent studies. Mar. Pollut. Bull. 133, 191–208. https://doi.org/10.1016/j.marpolbul.2018.05.022.

Rodriguez-Seijo, A., Lourenco, J., Rocha-Santos, T.A.P., da Costa, J., Duarte, A.C., Vala, H., Pereira, P., 2017. Histopathological and molecular effects of microplastics in Eisenia andrei Bouche. Environ. Pollut. 220, 495–503. https://doi.org/10.1016/j.envpol.2016.09.092.

Reid, B.J., Jones, K.C., Semple, K.T., 2000. Bioavailability of persistent organic pollutants in soils and sediments-a perspective on mechanisms, consequences and assessment. Environ. Pollut. 108 (1), 103–112. https://doi.org/10.1016/S0269-7491(99)00206-7.

Sarker, A., Deepo, D.M., Nandi, R., Rana, J., Islam, S., Rahman, S., Hossain, M.N., Islam, M.S., Baroi, A., Kim, J.-E., 2020. A review of microplastics pollution in the soil and terrestrial ecosystems: a global and Bangladesh perspective. Sci. Total Environ. 733, 139296. https://doi.org/10.1016/j.scitotenv.2020.139296.

Sanchez, W., Burgeot, T., Porcher, J.-M., 2013. A novel "integrated biomarker response" calculation based on reference deviation concept. Environ. Sci. Pollut. Res. 20 (5), 2721–2725. https://doi.org/10.1007/s11356-012-1359-1.

Song, Y.K., Hong, S.H., Jang, M., Han, G.M., Jung, S.W., Shim, W.J., 2018. Combined effects of UV exposure duration and mechanical abrasion on microplastic fragmentation by polymer type. Environ. Sci. Technol. 52, 3831–3832. https://doi.org/10.1021/acs.est.8b00172.

Song, X., Lyu, M., Zhang, X., Ruthensteiner, B., Ahn, I.-Y., Pastorino, G., Wang, Y., Gu, Y., Ta, K., Sun, J., Liu, X.i., Han, J., Ke, C., Peng, X., 2021. Large plastic debris dumps: new biodiversity hot spots emerging on the deep-Sea floor. Environ. Sci. Technol. Lett. 8 (2), 148–154. https://doi.org/10.1021/acs.estlett.0c00967.

Shao, Y.T., Wang, J., Du, Z.K., Li, B., Zhu, L.S., Wang, J.H., Zhang, S.M., 2018. Toxic effect of [Omim]BF4 and [Omim]Br on antioxidant stress and oxidative damage in earthworms (Eisenia fetida). Environ. Toxicol. Pharmacol. 60, 37–44. https://doi.org/10.1016/j.etap.2018.04.008.

Shi, X.J., Zhou, S.B., 2010. The role of Nrf2 and MAPK pathways in PFOS-induced oxidative stress in zebrafish embryos. Toxicol. Sci. Off. J. Soc. Toxicol. 115, 391–400. https://doi.org/10.1093/toxsci/kfq066.

Wang, J., Li, J.Y., Liu, S.T., Li, H.Y., Chen, X.C., Peng, C., Zhang, P.P., Liu, X.H., 2021. Distinct microplastic distributions in soils of different land-use patterns: A case study of Chinese farmlands. Environ. Pollut. 269, 116199 https://doi.org/10.1016/j.envpol.2020.116199.

Watts, A.J.R., Urbina, M.A., Corr, S., Lewis, C., Galloway, T.S., 2015. Ingestion of plastic microfibers by the crab Carcinus maenas and its effect on food consumption and energy balance. Environ. Sci. Technol. 49 (24), 14597–14604. https://doi.org/10.1021/acs.est.5b04026.

Watts, A.J.R., Urbina, M.A., Goodhead, R., Moger, J., Lewis, C., Galloway, T.S., 2016. Effect of microplastic on the gills of the shore crab Carcinus maenas. Environ. Sci. Technol. 50 (10), 5364–5369. https://doi.org/10.1021/acs.est.6b01187.

Wang, C.X., Zhang, Q.M., Liang, W.X., Wang, F.F., 2017. Toxicological effects of dimethomorph on soil enzymatic activity and soil earthworm (Eisenia fetida). Chemosphere 169, 316–323. https://doi.org/10.1016/j.chemosphere.2016.11.090.

Wang, W., Ge, J., Yu, X., Li, H., 2020a. Environmental fate and impacts of microplastics in soil ecosystems: Progress and perspective. Sci. Total Environ. 708, 134841. https://doi.org/10.1016/j.scitotenv.2019.134841.

Wang, Z., Yeung, K.W.Y., Zhou, G.-J., Yung, M.M.N., Schlekat, C.E., Garman, E.R., Gissi, F., Stauber, J.L., Middleton, E.T., Lin Wang, Y.Y., Leung, K.M.Y., 2020b. Acute and chronic toxicity of nickel on freshwater and marine tropical aquatic organisms. Ecotoxicol. Environ. Saf. 206, 111373. https://doi.org/10.1016/j.ecoenv.2020.111373.

Wang, X., Zheng, H., Zhao, J., Luo, X., Wang, Z., Xing, B., 2020c. Photodegradation elevated the toxicity of polystyrene microplastics to grouper (Epinephelus moara) through disrupting hepatic lipid homeostasis. Environ. Sci. Technol. 54 (10), 6202–6212. https://doi.org/10.1021/acs.est.9b0701610.1021/acs.est.9b07016.s001.

Wu, S., Wu, E., Qiu, L., Zhong, W., Chen, J., 2011. Effects of phenanthrene on the mortality, growth, and anti-oxidant system of earthworms (Eisenia fetida) under laboratory conditions. Chemosphere 83 (4), 429–434. https://doi.org/10.1016/j.chemosphere.2010.12.082.

Wu, X., Tong, Z.-H., Li, L.-L., Yu, H.-Q., 2013. Toxic effects of imidazolium-based ionic liquids on Caenorhabditis elegans: The role of reactive oxygen species. Chemosphere 93 (10), 2399–2404. https://doi.org/10.1016/j.chemosphere.2013.08.040.

Xu, B., Liu, F., Cryder, Z., Huang, D., Lu, Z., He, Y., Wang, H., Lu, Z., Brookes, P.C., Tang, C., Gan, J., Xu, J., 2020. Microplastics in the soil environment: Occurrence, risks, interactions and fate – A review. Crit. Rev. Environ. Sci. Technol. 50 (21), 2175–2222. https://doi.org/10.1080/10643389.2019.1694822.

Yang, Y., Liu, W., Zhang, Z., Grossart, H.-P., Gadd, G.M., 2020. Microplastics provide new microbial niches in aquatic environments. Appl. Microbiol. Biotechnol. 104 (15), 6501–6511. https://doi.org/10.1007/s00253-020-10704-x.

Zheng, Y.F., Li, J.X., Cao, W., Liu, X.H., Jiang, F.H., Ding, J.F., Yin, X.F., Sun, C.J., 2019. Distribution characteristics of microplastics in the seawater and sediment: A case study in Jiaozhou Bay, China. Sci. Total Environ. 674, 27–35. https://doi.org/10.1016/j.scitotenv.2019.04.008.

Zhu, B.K., Fang, Y.M., Zhu, D., Christie, P., Ke, X., Zhu, Y.G., 2018. Exposure to nanoplastics disturbs the gut microbiome in the soil oligochaete Enchytraeus crypticus. Environ. Pollut. 239, 408–415. https://doi:10.1016/j.envpol.2018.04.017.

Zhu, X.L., Zhao, W.H., Chen, X.H., Zhao, T., Tan, L.J., Wang, J.T., 2020. Growth inhibition of the microalgae Skeletonema costatum under copper nanoparticles with microplastic exposure. Mar. Environ. Res. 158, 105005. https://doi:10.1016/j.marenvres.2020.105005.

Zhou, J., Gui, H., Banfield, C.C., Wen, Y., Zang, H., Dippold, M.A., Charlton, A., Jones, D. L., 2021. The microplastisphere: Biodegradable microplastics addition alters soil microbial community structure and function. Soil Biol. Biochem. 156, 108211. https://doi.org/10.1016/j.soilbio.2021.108211.

Zhu, K., Jia, H., Zhao, S., Xia, T., Guo, X., Wang, T., Zhu, L., 2019. Formation of environmentally persistent free radicals on microplastics under light irradiation. Environ. Sci. Technol. 53 (14), 8177–8186. https://doi.org/10.1021/acs.est.9b01474.

Supplementary material

The protective layer formed by soil particles on plastics decreases the toxicity of polystyrene microplastics to earthworms *(Eisenia fetida)*

Jinbo Liu [a], Jianjun Qin [a], Lang Zhu [a], Kecheng Zhu [a], Ze Liu [a], Hanzhong Jia [a] *,
Eric Lichtfouse [b]

[a] Key Laboratory of Plant Nutrition and the Agri-environment in Northwest China, Ministry of Agriculture, College of Natural Resources and Environment, Northwest A & F University, Yangling 712100, China
[b] Aix-Marseille Univ, CNRS, IRD, INRA, CEREGE, Aix-en-Provence 13100, France

* Corresponding author   E-mail: jiahz@nwafu.edu.cn

Text S1 The size and composition of the PS-MP were analyzed by scanning electron microscopy (SEM, S-3400N, Hitachi, Japan) and attenuated total reflectance-fourier transform infrared spectroscopy (ATR-FTIR, Thermo Nicolet IS10, Massachusetts, USA), respectively. For metal contents, PS-MP were completely digested by microwave using the Aqua Regia solution of 3/1 37%HCl / 97%HNO$_3$. Concentration of metal ions in digestion solutions was measured by an inductively coupled plasma atomic emission spectrometer (ICP-AES) from Thermo-ICAP6300, Waltham. PS-MP were analyzed for their elemental carbon (EC) contents on an elemental analyzer (Vario MACRO cube, Elementar, Germany). Organic carbon (OC) and inorganic carbon (IC) in PS-MP were measured using a TOC analyzer (vario toc, Elementar, Germany). The metal contents of PS-MP were analyzed using an inductively coupled plasma mass spectrometry (ICP-MS, ICAP Qc, Thermo, USA). Specifically, 0.1 g of each PS-MP was predigested for 4 h in nitric acid (5 mL, 85%), which was subjected to microwave digestion in H$_2$O$_2$ (2 mL, 30%) for 1.5 h. Then, 2 mL of perchloric acid (70%) was added into the mixed solution, followed by heat digestion at 200 °C for 0.5 h. After cooling, the obtained solution was diluted to 100 mL and was filtered for ICP-MS analysis.

Text S2 The content of OC was measured using a total organic carbon (TOC) analyzer from Elementar vario series, Hesse-Darmstadt. The contents of clay, silt and sand were detected using laser particle size analyzer (Mastersizer 2000E). For pH determination, a 1/5 w/v mixture of soil in Milli-Q water with soil and solution was placed into a shaker for 1h, then settled before measuring pH. Cation exchange capacity (CEC) was obtained by adding 0.2 M NH$_4$Cl to substitute exchangeable cations, such as K$^+$, Na$^+$, Ca^{2+}, Mg^{2+}, Al^{3+}, into supernatant from the three consecutive washes, then were analyzed by ICP-AES.

Text S3 Briefly, 30% H_2O_2 was mixed with earthworm casts in beakers for 24 h at 50 °C to digest organic matter. The beakers were kept at 60 °C for 48 h for desiccation. For density flotation, a saturated NaCl solution (26%, w/v) was then added in the beakers, sonicated for 1 h, stirred for 30 min, and settled for 24 h. The supernatant containing PS-MP was transferred to another beaker. The steps of density flotation were repeated three times. The supernatants were gathered then filtered through a whatman glass microfiber filter paper (0.45 μm, GF/A). The retained PS-MP was transferred into a glass slide. Approximately 2–3 drops of a Nile red solution (1 mg/mL in methanol) were dropped to cover glass slide. The glass slide was kept in the dark at 60 °C for 10 min then observed using a laser scanning confocal microscope (LSCM, FV3000, Japan) at excitation/emission 561/570–670 nm.

Text S4 Earthworms were washed with 0.9% saline solution and fixed in 3–5 ml 14% glutaraldehyde for 30 min, rinsed with 1 ml potassium phosphate buffer saline (PBS, 0.1M, pH=7.4) and dehydrated with 50%, 70%, 90%, and 100% (wt%) ethanol solutions, with 10 min for each gradient. 1 ml isoamyl acetate was added for settling 10 min, and the earthworms were freeze-dried for 4 h using a LGJ-10C freeze-dryer, Karaltay Instruments Co., Ltd., Beijing, China. After pretreatment, earthworms were sprayed with an ion sputter coating apparatus (MSP-IS, Hitachi, Japan), and observed by scanning electron microscopy (SEM, S-3400N, Hitachi, Japan).

Text S5 At different aging periods, 50 g soils were moved into 500 mL glass beaker containing 100 mL saturated NaCl solution. The mixture was stirred for 10 min, and then centrifuged for 10 min at 8,000 × g. The supernatants were filtered through a cellulose membrane with a pore size of 0.25 μm. The final attached PS-MP filter membranes were stored in glass Petri dishes and left to dry at room temperature to obtain PS-MP.
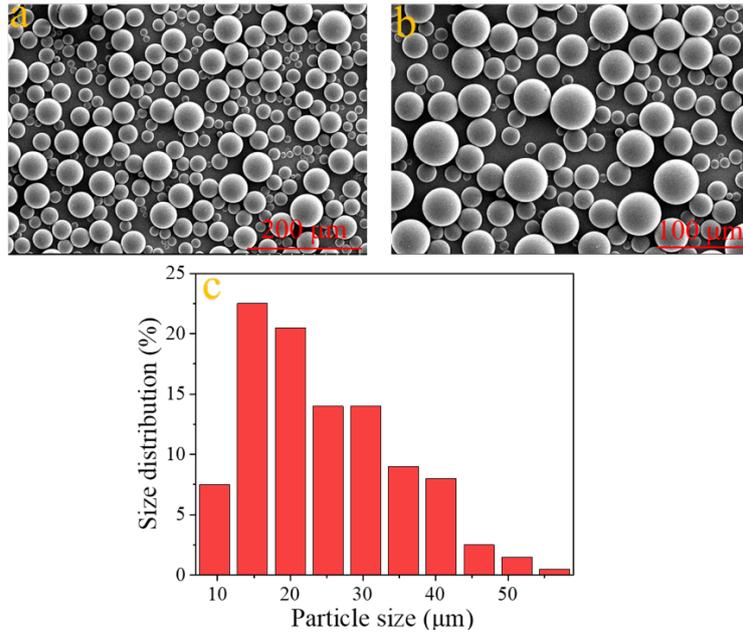
Fig. S1. Scanning electron microscope (SEM) images for PS-MP and particle size analyze using Nano measure 1.2
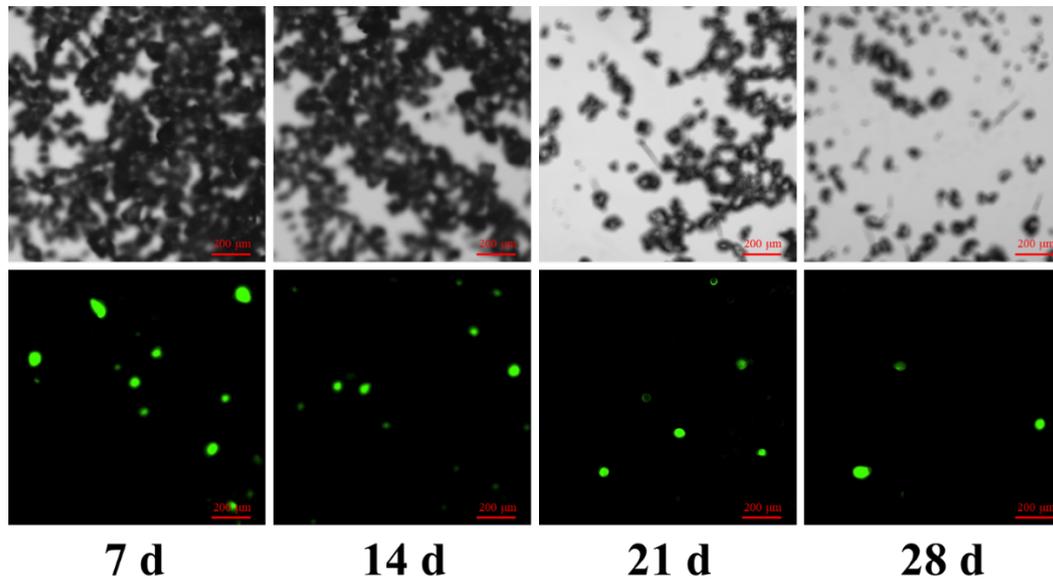

Fig. S2. The ingestion of different aging times of PS-MP by earthworms. The green dots were PS-MP, which decreased with the aging.
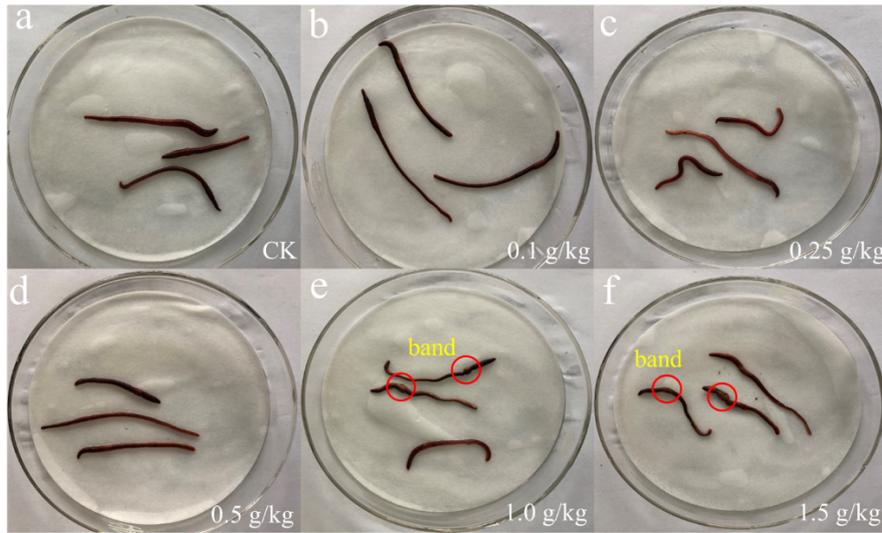
Fig. S3. Toxic symptoms of earthworms under PS-MP exposure with different concentrations. The physical damage, such as band swelling and pustule, was observed under 1.0 and 1.5 g kg^{-1} PS-MP
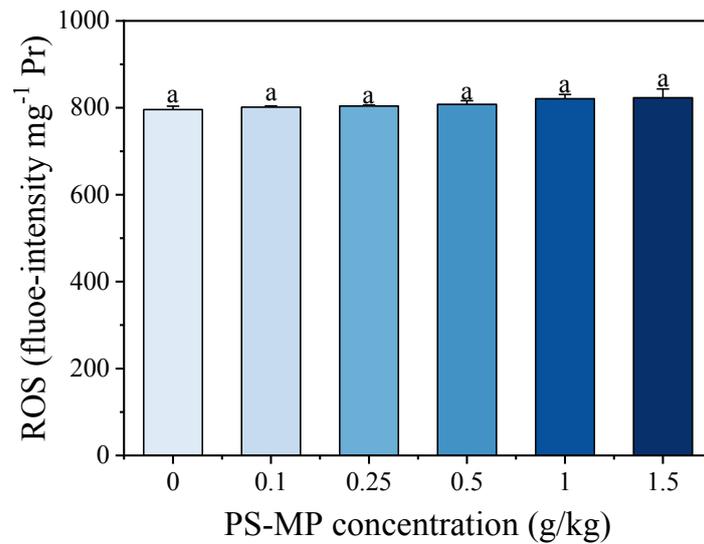

Fig. S4. The concentration of reactive oxygen species (ROS) in earthworms after exposure to different concentrations of aging polystyrene microplastic (PS-MP) for 7 days. The values are presented as the mean ± SD (n = 3), and the error bars represent the standard deviation. Different letters above columns indicate significant differences at $p < 0.05$ level among treatments.

Fig. S5. The biochemical indicators in earthworms after exposure to 1.5 g kg^{-1} PS-MP at different aging time for 7 days. (a) reactive oxygen species (ROS) level; (b) superoxide dismutase (SOD) activity; (c) catalase (CAT) activity; (d) peroxidase (POD) activity; (e) glutathione-S-transferase (GST) activity; (f) malondialdehyde (MDA) content and (g) integrated biomarker response (IBR) value. The values are presented as the mean ± SD (n = 3), and the error bars represent the standard deviation. Different letters above columns indicate significant differences at $p < 0.05$ level among treatments.
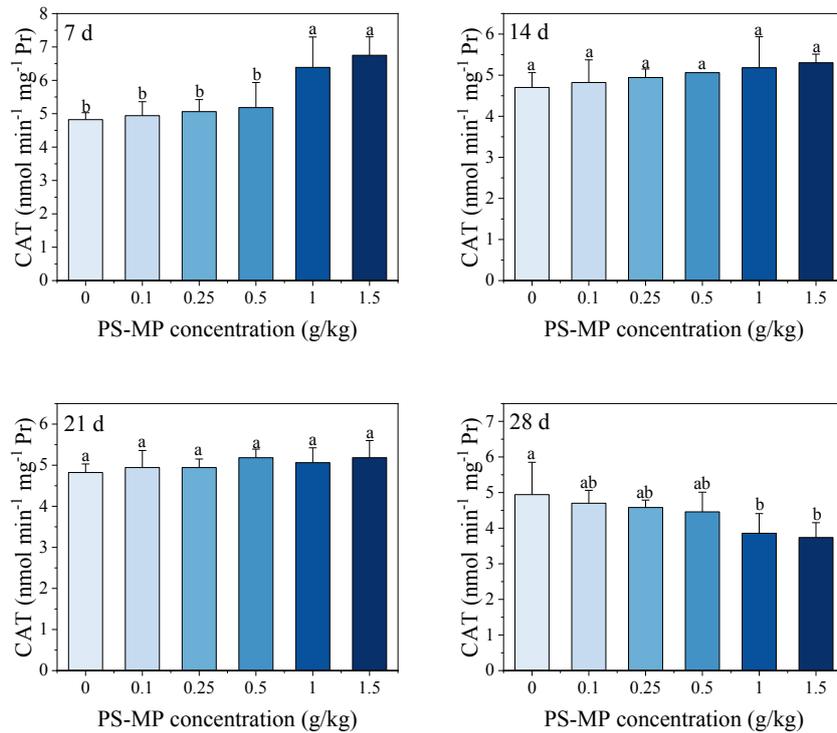
Fig. S6. Catalase (CAT) activity in earthworms after 7, 14, 21, 28 days exposure in soils amended with PS-MP. The values are presented as the mean ± SD (n = 3), and the error bars represent the standard deviation. Different letters above columns indicate significant differences at $p < 0.05$ level among treatments.
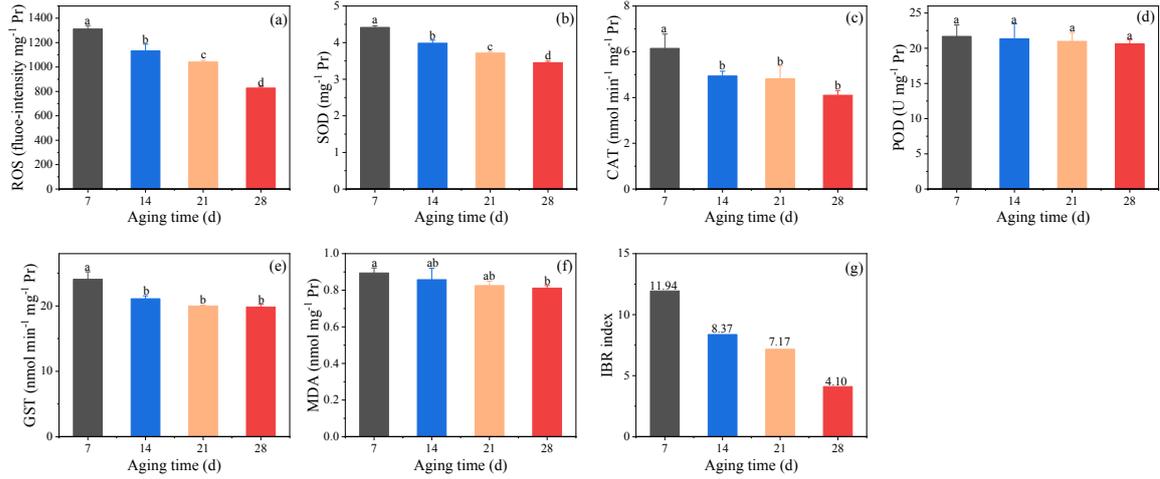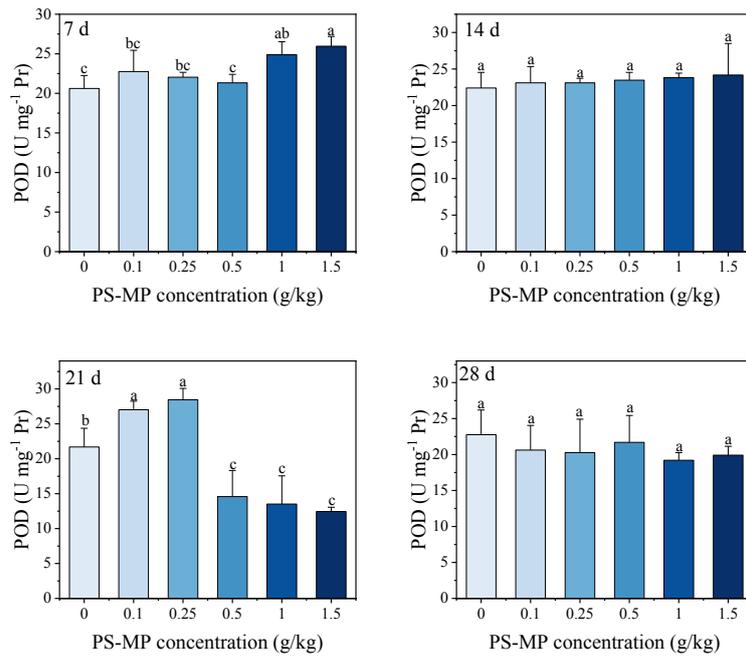
Fig. S7. Peroxidase (POD) activity in earthworms after 7, 14, 21, 28 days exposure in soils amended with PS-MP. The values are presented as the mean ± SD (n = 3), and the error bars represent the standard deviation. Different letters above columns indicate significant differences at $p < 0.05$ level among treatments.

Fig. S8. The glutathione-S-transferase (GST) activity in earthworms after 7, 14, 21, 28 days exposure to PS-MP at various concentrations in soils. The values are presented as the mean ± SD (n = 3), and the error bars represent the standard deviation. Different letters above columns indicate significant differences at $p < 0.05$ level among treatments.
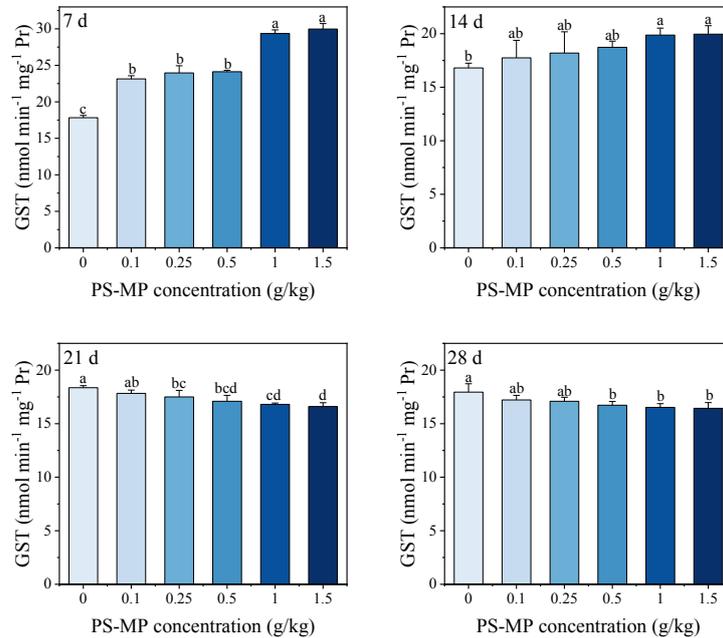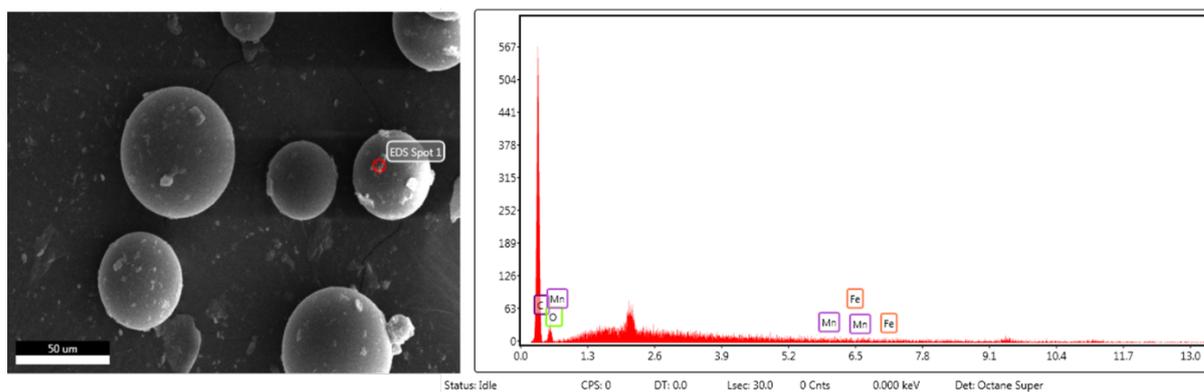
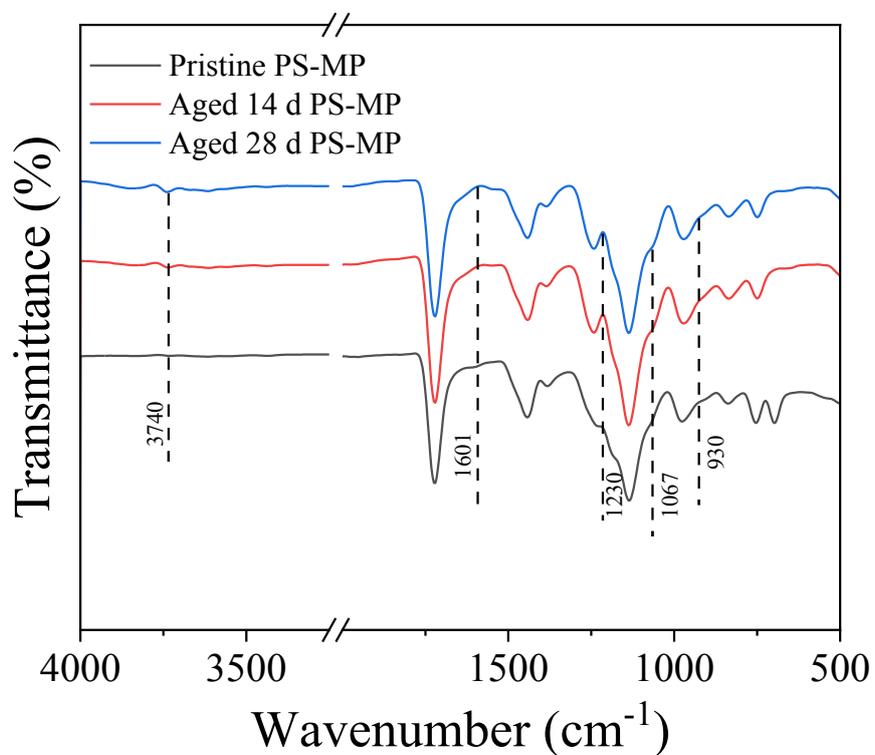**Fig. S9.** SEM-EDX images of aged PS-MP.

Fig. S10. ATR-FTIR spectra of PS-MP aging for different times, i.e., 0, 14 and 28 days.
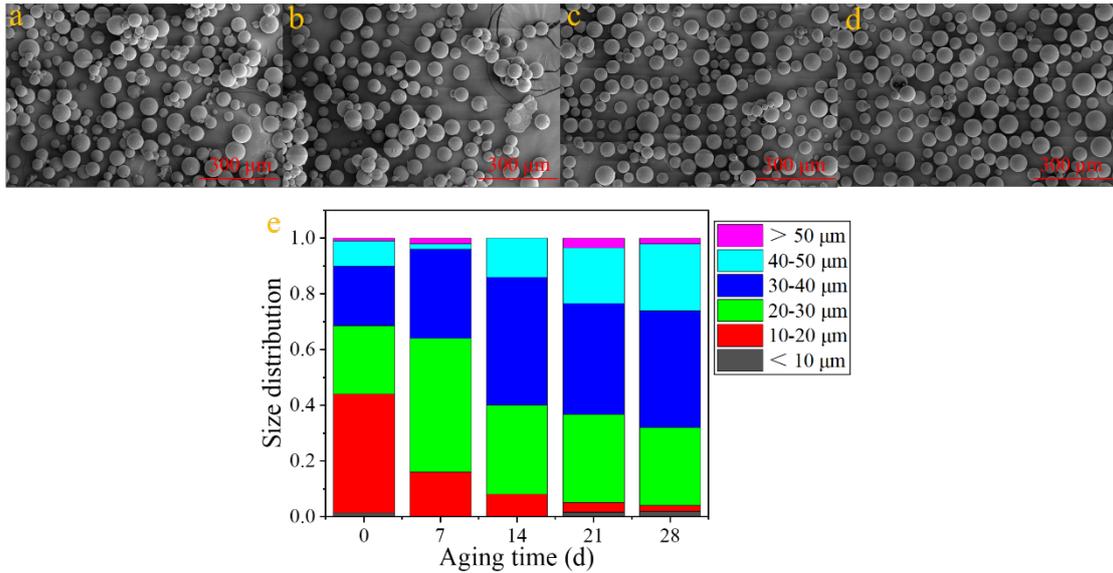
Fig. S11. SEM images of PS-MP aged for 7 days (a), 14 days (b), 21 days (c) and 28 days (d), and the size distribution of PS-MP with different aging times (e). All particles in the SEM images were measured by using a Nano Measurer to obtain the size distribution.

Table S1. Settings of the acute toxicity assay on earthworms

	Soil (g)	Vermiculite (g)	PS-MP (g)	Concentration of PS-MP (g/kg)
Control	450	50	0	0
T1	448	50	2	4
T2	445	50	5	10
T3	440	50	10	20
T4	430	50	20	40
T5	420	50	30	60
T6	410	50	40	80
T7	400	50	50	100

Table S2. Settings of the subchronic toxicity assay on earthworms

	Soil (g)	Vermiculite (g)	PS-MP (g)	Concentration of PS-MP (g/kg)
Control	450	50	0	0
T1	449.95	50	0.05	0.1
T2	449.875	50	0.125	0.25
T3	449.75	50	0.25	0.5
T4	449.5	50	0.5	1.0
T5	449.25	50	0.75	1.5

Table S3. Results of two-way analysis of variance for biochemical responses in earthworms (*Eisenia fetida*) treated with PS-MP

Biomakers	Dose			Time			Dose*Time		
	df[a]	F	P	df[a]	F	P	df[a]	F	P
ROS	5	392.500	0.000*	3	1286.289	0.000*	15	115.617	0.000*
SOD	5	377.473	0.000*	3	1234.880	0.000*	15	63.494	0.000*
CAT	5	1.468	0.218	3	17.155	0.000*	15	3.782	0.000*
POD	5	4.231	0.003*	3	9.154	0.000*	15	7.682	0.000*
GST	5	28.931	0.000*	3	443.494	0.000*	15	32.460	0.000*
MDA	5	25.679	0.000*	3	12.891	0.000*	15	3.504	0.000*

[a] df, degrees of freedom, * $p < 0.05$.

Table S4. Results of the post hoc test using LSD[a] after two-way ANOVA[b] for the tested biomarkers in earthworms (*Eisenia fetida*) treated with PS-MP

Biomakers	Dose (g kg^{-1}) [c,*]						Time (d) [c,*]			
	0	0.1	0.25	0.5	1.0	1.5	7	14	21	28
ROS	a	b	c	d	e	e	a	b	c	c
SOD	a	b	ce	d	e	e	a	b	c	d
CAT	a	ab	ab	ab	ab	b	a	bc	c	d
POD	abc	a	ab	c	c	c	a	a	b	b
GST	a	b	b	b	c	c	a	b	c	c
MDA	a	b	c	cd	d	d	a	b	a	b

[a] LSD, least significant difference.

[b] ANOVA, analysis of variance.

[c] Different letters indicate significant differences among different doses or time, * $p < 0.05$.

Table S5. The relative contents of PS-MP elements in pristine and different aging times.

Samples	Element Weight (%)				
	C	O	Fe	Mn	O+Fe+Mn
Pristine PS-MP	86.13	12.74	0.67	0.46	13.87
Aging 7 d PS-MP	84.16	14.39	0.74	0.71	15.84
Aging 14 d PS-MP	81.18	18.21	0.33	0.28	18.82
Aging 21 d PS-MP	77.40	21.86	0.37	0.37	22.60
Aging 28 d PS-MP	73.81	25.74	0.30	0.15	26.19